Effects of nilotinib on leukaemia cells using vibrational microspectroscopy and cell cloning

Siddique M. R.[1], Rutter A. V.[1], Wehbe K.[2], Cinque G.[2], Bellisola G.[3] and Sulé-Suso J.[1,4]

[1] Institute for Science and Technology in Medicine
Keele University
Guy Hilton Research Centre
Thornburrow Drive
Stoke on Trent ST4 7QB
U. K.

[2] Diamond Light Source, Harwell Science and Innovation Campus
Didcot,
Oxfordshire, OX11 0DE
U. K.

[3] University Hospital of Verona
Department of Pathology and Diagnostics
Unit of Immunology
Policlinico G. Rossi
P.le L.A. Scuro, 10
I-37134 Verona
Italy

[4] Oncology Department
Royal Stoke University Hospital
University Hospitals of North Midlands (UHNM)
Newcastle Rd
Stoke on Trent
Staffordshire ST4 6QG
U. K.

Keywords: Leukaemia; Fourier Transform Infrared Microspectroscopy; Raman Microspectroscopy; Synchrotron; Cell Cloning; Nilotinib.

Abstract

Over the last few years, both synchrotron-based FTIR (S-FTIR) and Raman microspectroscopies have helped to better understand the effects of drugs on cancer cells. However, cancer is a mixture of cells with different sensitivity/resistance to drugs. Furthermore, the effects of drugs on cells produce both chemical and morphological changes, the latter could affect the spectra of cells incubated with drugs. Here, we successfully cloned sensitive and resistant leukaemia cells to nilotinib, a drug used in the management of leukaemia. This allowed both the study of a more uniform population and the study of sensitive and resistant cells prior to the addition of the drug with both S-FTIR and Raman microspectroscopies. The incubation with nilotinib produced changes in the S-FTIR and Raman spectra of both sensitive and resistant clones to nilotinib. Principal Component Analysis was able to distinguish between cells incubated in the absence or presence of the drug, even in the case of resistant clones. The latter would confirm that the spectral differences between the so-called resistant clonal cells prior to and after adding a drug might reside on those more or less sensitive cells that have been able to remain alive when they were collected to be studied with S-FTIR or Raman microspectroscopies. The data presented here indicate that the methodology of cell cloning can be applied to different types of malignant cells. This should facilitate the identification of spectral biomarkers of sensitivity/resistance to drugs. The next step would be a better assessment of sensitivity/resistance of leukaemia cells from patients which could guide clinicians to better tailor treatments to each individual patient.

Introduction

Chronic myelogenous leukaemia (CML), a bone marrow stem cell disease, accounts for approximately 10%-15% of all leukaemia cases. The reciprocal translocation between chromosomes 22 and 9 allows the generation of the chimeric *bcr-abl* fusion gene, the so-called Philadelphia chromosome. This acquired genetic aberration can be observed in 95% of CML patients[1]. The molecular defect resides in the abnormal tyrosine kinase activity of the kinase domain in the resulting *bcr-abl* protein. As a consequence, downstream target proteins become hyper-phosphorylated and their homeostatic control is undermined allowing stem cell growth to become independent of the action of cell growth factors and insensitive to pro-apoptotic stimuli. The outcome is both increased cell proliferation and resistance to apoptosis of CML stem cell population which progressively expands in the bone marrow[2, 3]. These features make the kinase domain of *bcr-abl* protein an important target in the development of anti-leukaemic drugs which include amongst others imatinib, nilotinib and dasatinib[4]. Imatinib was the first to be developed and this leading compound still represents the first choice in the treatment of CML patients. However, drug-resistance is a problem. Therefore, great efforts are being placed to develop new tyrosine kinase inhibitor (TKI) molecules in an attempt to induce cytogenetic remission and/or delay the onset of drug-resistance in CML patients.

Presently, the therapeutic follow-up of CML makes use of available clinical laboratory tests that quantify residual disease in CML patients[5]. The kinase domain mutation analysis allows to predict/assess cancer cells' sensitivity/resistance to anti-leukaemic

drugs[6]. However, there are still two major issues in the management of leukaemia. First, the anti-leukaemic strategy is mainly based on protocols tested in multicentre studies and, at present, it is not possible to establish “a priori” the best drug and/or combination of drugs for each individual patient. Second, the systematic analysis of abl kinase domain mutations is not a reliable and economically convenient approach to ascertain what tumour cell clones will develop drug resistance. In fact, the Philadelphia chromosome is characterized by its intrinsic hyper-mutability allowing the monitoring of kinase domain mutations most likely unfeasible[7]. In addition, there is high phenotypic variability within cells of a given tumour and leukaemic clones will contain sub-clones with different unpredictable grades of sensitivity/resistance to TKIs[8].

Vibrational microspectroscopy has been applied to study leukaemia cells’ sensitivity/resistance to drugs *in vitro*[9-21] and to assess/monitor therapeutic responses in patients with leukaemia[22-24]. All these studies have proven that vibrational spectroscopy, performed either with FTIR or Raman techniques, is sensitive enough to identify some biochemical signatures related to the effects of different anti-leukemic drugs. However, one of the limitations of those studies is that most probably the presence of both drug-sensitive and drug-resistant cell clones and all the possible variations in-between in those samples was not appropriately taken into account. The uncertainty regarding the relative fractions of sensitive and resistant cells in the sample can limit the results’ interpretation, in particular when the IR spectra are an average of signals from cells with different phenotypes[16]. Therefore, it is important when assessing cell sensitivity/resistance to drugs using vibrational spectroscopy to be carried out with samples containing cells with a

uniform phenotype[25]. Cell sub-cloning is a recently applied strategy to explore the infrared identification of gemcitabine-sensitivity/resistance in more cell homogeneous samples exposed to a drug[26].

The present work aims at assessing whether combining cell sub-cloning and principal component analysis (PCA) of both FTIR and Raman spectra datasets is an appropriate approach that could be extended to test and predict drug-resistance/sensitivity in leukaemic cells. Leukaemia is thus an excellent example to assess this methodology with a clinical application thanks to the ease of obtaining leukemia cells from the peripheral blood of CML patients. In order to identify possible spectral markers of sensitivity/resistance, chronic myelogenous leukaemia cell clones were analysed prior to and after the addition of nilotinib. Both, synchrotron based FTIR (S-FTIR) and Raman microspectroscopy were used in this study. Nilotinib is an effective second generation TKI molecular compound developed to overcome imatinib resistance in leukaemic cells[27, 28] and showing greater efficacy than imatinib[29]. However, some leukaemia cells still display significant resistance to nilotinib[30].

Materials and Methods

Cell line

The K562 chronic myelogenous leukaemia cell line, a widespread model of human CML utilized for the *ex vivo* testing/screening of drugs, was used in this study. Cells were grown in suspension in RPMI 1640 culture medium supplemented with 10%

Foetal Bovine Serum, 1% L-Glutamine, 1% Hepes Buffer, and 1% Antibiotic/antimycotic (complete medium) in culture flasks (Sarstedt, UK) at 37°C and 5% CO_2. The growth medium was changed every 3-4 days and cells were split 1:3. Cell viability was determined with the standard trypan blue exclusion method.

Cell cloning

Cells were expanded in 75 cm^2 culture flasks (Sarstedt, UK), transferred to 50 mL conical tubes and centrifuged at 950 rpm for 3 minutes. The supernatant was discarded and the cell pellet was dislodged and re-suspended in fresh complete medium. Cells were then counted using the trypan blue exclusion assay. Living cells were appropriately diluted in complete medium and seeded in flat-bottomed 96 well plates at a concentration of 0.5 cells/200 µL/well (example and for simplicity, for 100 wells, 50 cells were placed in 20 mL of medium and distributed evenly in these 100 wells). The plates were incubated at 37°C and in a 5% CO_2 atmosphere. Following one week culture, the plates were spun at 1200 rpm for 7 minutes. Following this, 100 µL of medium were removed and 100 µL of fresh complete medium were added. Plates were further incubated at 37°C and 5% CO_2 for one week to allow the clones to develop. Clones were inspected regularly so those wells with more than 1 clone could be discarded. After these 2 weeks culture, between 15 and 20 clones grew per each 96 well plate. In order to study as many cells as possible for each individual clone, especially those grown in the presence of nilotinib, the number of cells for each individual clone were not counted.

Nilotinib

Nilotinib (a kind gift of Novartis, Switzerland) was provided in powder form (100 mg) and dissolved in DMSO to a final concentration of 10 mM according to the provider's instructions. Aliquots were stored at -20 °C. Nilotinib was added to cells as follows. After 2 weeks culture in 96 well plates as described above, clones were collected by gently mixing the media in each individual well containing an individual clone and collecting both the total media (200 µL) and cells. For each individual clone, cells were seeded proportionally in 3 wells in 96 flat-bottomed plates. They were allowed to grow for a further 24 hours at 37 °C and 5% CO_2. Following this incubation period, plates were spun at 1200 rpm for 7 minutes. Following this, 100 µL of growth medium were removed and 100 µL of fresh medium with different concentrations of nilotinib were added (final concentrations of 0 µM, 50 µM or 100 µM). Cells were then allowed to grow for 5 days at 37 °C and 5% CO_2 in order to assess clone cell growth. Preliminary work was carried out to optimise time-course and dose-response experiments with nilotinib. It was observed that keeping cells growing for more than 5 days translated into cells overgrowing in control wells (in the presence of 0 µM nilotinib). On the other hand, clones grew in the presence of 10 µM nilotinib, and all clones died at 5 days culture in the presence of 500 µM nilotinib. Therefore, the doses of 0 µM, 50 µM and 100 µM nilotinib and an incubation time of 5 days were established in this study. In order to assess cell survival in the absence or presence of nilotinib which decreases cell viability in a time, dose and growth condition dependent manner, clones that grew to confluence (cells occupied the whole surface of the well) were labelled "++" and those clones that grew to semi-confluence (cells did not occupy the whole surface of the well) were labelled "+". Wells that contained just few cells were labelled "+/-". Finally, those wells which contained no cells were

labelled "-." Table I shows a representative example of clones obtained from one 96 well plate.

Vibrational Microspectroscopy

Sample preparation. Following cell incubation in the absence or presence of nilotinib, cells were collected, transferred into Eppendorf tubes and centrifuged at 950 rpm for 3 minutes at room temperature. Supernatant was then removed and the pelleted cells were re-suspended in 0.9% NaCl. Cells were then cytospun on CaF_2 slides for 1 minute at 550 rpm and fixed with 4% buffered paraformaldehyde in 0.9% NaCl for 20 min at room temperature. Excess formalin was removed by washing once with NaCl 0.9% and thrice rinsed with distilled water. Samples were then air dried at room temperature[31]. UV graded CaF_2 slides (26 x 22 x 0.5 mm) (Crystan Ltd, UK) suitable for both FTIR and Raman microspectroscopy were used. Spectra of 50 individual cells were obtained from control and nilotinib-resistant clones while this number was reduced in samples that resulted sensitive to nilotinib (see Figures' legends).

S-FTIR microspectroscopy. S-FTIR spectra were recorded in transmission mode at MIRIAM beamline at Diamond Light Source, UK. The end station has a Hyperion 3000 microscope (Bruker) with a liquid nitrogen cooled 50 µm pitch high sensitivity MCT detector coupled to a Bruker 80V FTIR spectrometer. Opus (Bruker) software was used to record the FTIR spectra (and visible images) at 4 cm^{-1} resolution with 256 co-added scans. Based on our previous work[31], single cell IR data were taken in transmission mode using 15×15 µm slits via a 36x objective/condenser optics and centring onto the cell nucleus.

Pre-processing. IR spectra were corrected for baseline fluctuation using non-resonant Mie scattering extended multiplicative signal correction (EMSC)[32]. Following EMSC correction, the spectra were cropped to the fingerprint (1000-1800 cm^{-1}) and the lipid (2700–3100 cm^{-1}) regions and normalized using standard normal variate (SNV), which subtracts the mean spectrum and then divides by the standard deviation for each spectrum removing the effect of different sample thickness and spectrum baseline offsets. Afterwards, principal component analysis (PCA) was performed using Unscrambler X software (CAMO).

Raman spectroscopy. A Senterra Raman (Bruker) system was used off line at MIRIAM beamline at Diamond Light Source, equipped with 532 nm 100 mW laser and a Si CCD detector thermoelectrically cooled at -80 °C. Opus (Bruker) software was used to obtain the Raman microspectra and visible images via a 100x 0.8 NA low-fluorescence objective, with internal Neon lamp for spectral calibration. The spectra were recorded between 40 and 4450 cm^{-1} at resolution 9-18 cm^{-1} by co-adding 2 acquisitions (for cosmic ray removal) each of 10 seconds integration time. A 50 µm pinhole and total power of max 10 mW was used at the spectrograph entrance, in order to guarantee confocality and detectable Raman signal below the damaging threshold of the sample. Three spectra were recorded on different locations of each individual cell and averaged. Rubberband baseline correction was carried out followed by SNV normalization. PCA was performed using Unscrambler. As in the case of S-FTIR microspectra, Raman microspectra were obtained from the nuclear area based on our previous work showing that differences between cells reside mainly in the nucleus[31, 33]. For each clone, Raman spectra of 50 individual

control cells were obtained. Spectra of 50 individual cells were obtained from control and nilotinib-resistant clones while this number was reduced in samples that resulted sensitive to nilotinib (see Figures' legends).

RESULTS

The aim of this feasibility study was to identify possible IR and/or Raman spectral markers of nilotinib sensitivity/resistance in a clonal leukaemia cell population. Furthermore, sensitive and resistant clone cells were studied prior to the addition of the drug in order to obviate any morphological changes related to the pro-apoptotic effects of nilotinib that could affect their IR and/or Raman spectra. The beamtime at MIRIAM beamline was mainly dedicated to the study of the effects of nilotinib in clonal cells using S-FTIR microspectroscopy. We also took the opportunity to complement this work with Raman studies on the effects of nilotinib on clonal leukaemia cells.

The cloning of the K562 cell line yielded between 15 and 20 cell clones with different sensitivities to nilotinib per each 96 well plate. Table I shows a representative example of the clones obtained from a 96 well plate. It is obvious that even within an already well established cell line there are important phenotypical differences in the sensitivity/resistance of individual cells to nilotinib. This tumour variability could mask some of the spectral markers of cell sensitivity to a given drug if the spectra were taken from a mixed cell culture containing a higher number of resistant cells.

Following cell cloning and incubation with nilotinib, we studied the effects of nilotinib in a cell clone resistant to both 50 µM and 100 µM nilotinib i.e., at least 50 cells could be studied for each of the three doses of nilotinib (0 µM, 50 µM and 100 µM). We also chose a clone sensitive to 100 µM of nilotinib and semi-sensitive to 50 µM of nilotinib (only 23 cells could be studied when the cell clone was incubated with 50 µm of nilotinib). Figure 1 shows the mean spectra for clone 4F (resistant to both 50 µM and 100 µM of nilotinib). Even in a resistant clone, there are spectral changes following the addition of nilotinib. The differences reside mainly in the shape of the amide I and II bands (becoming broader following the addition of the drug) and a decrease in the intensity of the peaks at 1740 cm^{-1}, 2850 cm^{-1} and 2920 cm^{-1}. In the case shown in Figure 2, clone 7F (semisensitive/semiresistant to nilotinib) has again a broadening of the amide I and II bands. Here, there is a small increase in the intensity of the peaks at 1740 cm^{-1}, 2850 cm^{-1}, and 2920 cm^{-1}.

PCA of these 2 clones prior to and after the addition of nilotinib and corresponding plots can be seen in Figures 3 and 4 respectively. As can be seen in Figure 3, even in a resistant clone, some separation between control cells and those incubated with the drug could be seen both in the fingerprint and the lipid regions. More importantly, the separation was higher for the semisensitive/semiresistant clone between control cells and those cells incubated with 50 µM nilotinib.

On the other hand, the PCA of control cells (incubated with 0 μM nilotinib) for resistant and sensitive clones is shown in Figure 5. These clones are: resistant clones 2F, 3F and 4F to both 50 μM and 100 μM of nilotinib (crosses); sensitive clone 1F to both 50 μM and 100 μM nilotinib (filled triangles) and sensitive clones 5F and 7F to 100 μM nilotinib only (open circles). As can be seen in Figure 5, there was a clear separation between the control cells for the resistant clones and the control cells for the clone sensitive to both 50 μM and 100 μM nilotinib for both fingerprint and lipid regions. Furthermore, there was also some separation between control cells for resistant clones to both 50 μM and 100 μM of nilotinib and control cells for clones sensitive to 100 μM nilotinib only for both fingerprint and lipid regions.

Raman spectra of a resistant and a semiresistant/semisensitive clone were also obtained. Figure 6 shows the mean spectra of resistant clone 1Ra cells (resistant to both 50 μM and 100 μM of nilotinib) in the absence and in the presence of nilotinib at 50 μM and 100 μM. No major differences can be seen between control cells (incubated with 0 μM nilotinib) and cells incubated with 50 μM nilotinib apart from a decrease in the intensity of the peak at 1100 cm^{-1}. However, some changes can be seen in cells incubated with 100 μM nilotinib. These differences are mainly an increase in the intensity of the peaks at 965 cm^{-1} and 1610 cm^{-1}. On the other hand, Figure 7 shows the mean spectra of semiresistant/semisensitive clone 2Ra. In this case, only 25 cells could be seen following the incubation with 50 μM of nilotinib. Here, the main differences were a change in the ratios of peaks at 1315 cm^{-1} and 1335 cm^{-1}, and a decrease in the intensity of the peaks at 780, 1100, 1370, 1485, 1520 and 1580 cm^{-1}. Figures 8 and 9 show the PCA and corresponding plots prior to and after the addition of nilotinib for these 2 clones, respectively. It can be seen in

Figure 8 that even for resistant clones, a separation between control cells and those incubated with either 50 μM or 100 μM nilotinib could be seen. Furthermore, a clear separation could be observed between control cells and those incubated with 50 μM nilotinib for the semiresistant/semisensitive clone 2Ra cells (Figure 9).

DISCUSSION

The potential of vibrational spectroscopy as a tool which could help in the management of leukaemia to better tailor treatment to an individual patient is widely accepted based on the number of publications on the subject (see Introduction). However, before this technique makes it into clinical practice, a better understanding of tumour cell sensitivity/resistance to drugs is needed. Leukaemia, like solid tumours, is made up of a whole array of resistant/sensitive cells to different drugs and combinations of drugs. One way to have a better understanding of the percentage of resistant or sensitive cells to a given drug in a whole leukaemia population is to carry out cell cloning and use this methodology together with vibrational spectroscopy to assess the presence of spectral biomarkers of resistance/sensitivity to the drug. While we have already shown the proof of concept in lung cancer[26], it was important to us to assess whether the same methodology could also be applied to a different type of tumour such as leukaemia, and using a drug with a different mechanism of action (nilotinib). Table I not only gives a representative example of the feasibility of this methodology in leukaemia but also gives an indication of the number of resistant, semiresistant/semisensitive and sensitive clones to nilotinib that are present in a whole leukaemia cell population.

This clearly indicates that the studies of the effects of drugs in whole cancer cell populations might prove more difficult to identify possible spectral biomarkers of resistance/sensitivity to drugs due to cellular heterogeneity. Cell cloning could be a way to more easily characterise the possible presence of these spectral biomarkers in a cancer cell population.

The data presented here shows that even in the so-called resistant clones (resistant to both 50 μM and 100 μM of nilotinib) some differences can be seen when carrying out PCA (Figure 3). It has to be taken into account that, even in a resistant cell population, following the incubation with the drug, there will be cells that could have been damaged, and might be repairing this damage or entering the initial phase of apoptosis (programmed cell death). It could be hypothesised that the differences seen here in the resistant clone following the addition of nilotinib at 50 μM or 100 μM could be caused by the presence of these damaged cells that were still alive when the sample was collected to carry out S-FTIR or Raman microspectroscopy. Obviously, further work is needed to confirm this.

The main differences seen in the S-FTIR spectra of semiresistant/semisensitive cells was an increase in the intensity of the peaks at 2850 cm^{-1} and 2920 cm^{-1} corresponding mainly to CH_2 stretching modes of methylene chains in membrane lipids and the peak at 1740 cm^{-1} arising from the carbonyl C=O stretching mode of phospholipids[34, 35]. We and others have described this increased intensity in the lipid peaks following the addition of drugs to different cell types[18, 19, 26, 36-38] which could be a spectral marker of apoptosis as an increase in lipid content correlates with

apoptosis[12, 38, 39]. On the other hand, the intensity of these 3 peaks decreased following the addition of the drug to resistant cell clones (Figure 1). This is in agreement with previously reported data indicating an association between a decrease in lipids and drug resistance both in cell lines and in cells freshly isolated from leukemia patients[40]. However, it has also been described that there is a slight increase in intensity in the bands at 2854 cm^{-1} and 1740 cm^{-1} in imatinib resistant K562 leukaemia cells[20], an increase in the amount of unsaturated lipids in nilotinib resistant K562 cells[17] and a decrease in the intensity of the 1740 cm^{-1} band in imatinib sensitive K562 cells[21]. It is difficult to assess whether these reported results are different due to the fact that whole leukaemia cell populations were studied and/or resistant cell lines were created prior to studying the effects of drugs rather than studying the effects of a drug on a given clonal cell population. Furthermore, it has been described that some cells may have different rates of drug response indicating that not all drug exposed cells show a change in their spectra at a given incubation time[15]. This stresses the importance of studying a homogeneous cell population such as cell clones, to better assess possible spectral biomarkers of cell sensitivity/resistance to drugs.

Another important change in our cell clones following the addition of nilotinib was the decreased intensity and changes in the amides' region even for resistant cells (Figures 1 and 2). Changes in this region following the addition of drugs to leukaemia cells have also been previously reported[10, 14, 36, 41]. An important consideration in the study of cancer cells and their sensitivity to drugs would be to identify cell populations that could be sensitive or resistant to drugs prior to the addition of the drug. The data presented here (Figure 5) indicate that it is possible to separate, to a

certain extent, between nilotinib sensitive and resistant leukaemia cell clones. This was not the case in our previous work where no differences were seen between sensitive and resistant lung cancer cells clones[26]. However, it has to be taken into account that the differences might simply be due to the fact these are different clones. Further work is needed to assess whether different cell types could have different spectral markers of cell sensitivity to drugs.

On the other hand, Raman spectroscopy was also able to separate between cell clones in the absence or presence of nilotinib (Figure 6 and 7). For the sensitive cell clone, the main differences resided in an increase in the peak at 1335 cm^{-1} (CH vibrations)[42, 43], and a decrease in the peaks at 1370, 1485, 1520 cm^{-1} (all three due to adenine)[44]. However, for the resistant cell clone, while no major differences were seen between control cells (incubated with 0 µM nilotinib) and cells incubated with 50 µM nilotinib, there were differences when these cells were compared to cells incubated with 100 µM nilotinib, mainly at peaks 960 cm^{-1} (vibrational mode of proteins)[45], and 1610 cm^{-1} (tyrosine)[44]. The reason why changes in lipids were mostly seen when using FTIR microspectroscopy could be due to the way the experiments were implemented. In the case of FTIR microspectroscopy, the cell area covered was 15 x 15 µm while for Raman microspectroscopy was around 1 µm and focussed on the cell nucleus. An aperture of 15 x 15 µm would include most if not all of the cell and, thus, membrane lipids (with their corresponding changes mentioned above after the addition of the drug) while this would not be the case in Raman microspectroscopy. On the other hand, the spectral changes linked to DNA (decrease in the intensity of the adenine peaks in Raman and a decrease of the intensity of the peaks at 1080 cm^{-1} and 1240 cm^{-1} in FTIR) are due most probably to

apoptosis. It is well known that apoptosis causes nuclear fragmentation, membrane blebbing and release of apoptotic bodies leading, amongst other, to changes in cells' DNA. In fact, nilotinib not only binds to *bcr-abl* protein but also inhibits a broad spectrum of protein kinases which leads to apoptosis in several tumour cells including K562 leukaemia cells[46].

The data presented here indicate that the methodology of cell cloning can be applied to different types of malignant cells. Furthermore, it could represent a way forward to study the effects of drugs on more uniform cell populations. This should facilitate the identification of spectral biomarkers of sensitivity/resistance to drugs which otherwise could be partially masked in more heterogeneous cell populations. Further steps are needed to better understand how possible spectral biomarkers present in different cell clones correlate with a mode of death and/or different phases within the apoptosis process. The final aim would be to assess sensitivity/resistance of leukaemia cells from patients to better tailor treatment to each individual patient.

Acknowledgments

We thank Diamond Light Source for access to the MIRIAM beamline, B22, which contributed to the results presented here.

References

1. Rowley, J. D. *Nature*, 1973, **243,** 290-293.

2. Cortez, D., Stoica, G., Pierce, J. H., and Pendergast, A. M. *Oncogene*, 1996, **13**, 2589-2594.

3. Chopra, R., Strasser, A., Metcalf, D., and Elefanty, A. G. *Oncogene*, 1998, **16**, 335-348.

4. Emole, J., Talabi, T., and Pinilla-Ibarz, J. *Biologics,* 2016, **10,** 23-31.

5. Alikian, M., Ellery, P., Forbes, M., Gerrard, G., Kasperaviciute, D., Sosinsky, A., Mueller, M., Whale, A. S., Milojkovic, D., Apperley, J., Huggett, J. F., Foroni, L., and Reid, A. G. *J Mol Diagn*, 2016, **18,** 176-189.

6. Alikian, M., Gerrard, G., Subramanian, P. G., Mudge, K., Foskett, P., Khorashad, J. S., Lim, A. C., Marin, D., Milojkovic, D., Reid, A., Rezvani, K., Goldman, J., Apperley, J., and Foroni, L. *Am J Hematol*, 2012, **87,** 298-304.

7. Soverini, S., De Benedittis, C., Mancini, M., and Martinelli, G. *Oncologist*, 2016, **21,** 626-633.

8. Khorashad, J**.** S**.**, Deininger, M**.** W**.**, and O'Hare, T. *Oncotarget*, 2013, **4**, 7-8.

9. Le Gal, J. M., Morjani, H., and Manfait, M. *Cancer Res*, 1993, **53**, 3681-3686.

10. Liu, K.-Z., and Mantsch, H.H. *J Mol Structure*, 2001b, **565-566**, 299-304.

11. Gaigneaux, A., Ruysschaert, J. M., and Goormaghtigh, E. *Eur J Biochem*, 2002, **269,** 1968-1973.

12. Gault, N., and Lefaix, J.-L. *Radiat Res*, 2003, **160,** 238-250.

13. Liu, M. J., Wang, Z., Wu, R. C., Sun, Q., and Wu, Q. Y. *Leukemia*, 2003, **17,** 1670-1674.

14. Krishna, C. M., Kegelaer, G., Adt, I., Rubin, S., Kartha, V. B., Manfait, M., and Sockalingum, G. D. *Biopolymers*, 2006, **82**, 462-470.

15. Moritz, T. J., Taylor, D. S., Krol, D. M., Fritch, J., and Chan, J. W. *Biomed Opt Express*, 2010, **1**, 1138-1147.
16. Bellisola, G., Della Peruta, M., Vezzalini, M., Moratti., E., Vaccari, L., Birarda, G., Piccinini, M., Cinque, G., and Sorio, C. *Analyst*, 2010, **135**, 3077-3086.
17. Ceylan, C., Camgoz, A., and Baran, Y. *Technol Cancer Res Treat*, 2012, **11**, 333-344.
18. Machana, S., Weerapreeyakul, N., Barusrux, S., Thumanu, K., and Tanthanuch, W. *Talanta*, 2012, **93,** 371-382.
19. Travo, A., Desplat, V., Barron, E., Poychicot-Coustau, E., Guillon, J., Déléris, G., and Forfar, I. *Anal Bioanal Chem*, 2012, **404**, 1733-1743.
20. Baran, Y., Ceylan, C., and Camgoz, A. *Biomed Pharmacother*, 2013, **67**, 221-227.
21. Yandim, M. K., Ceylan, C., Elmas, E., and Baran, Y. *Tumor Biol*, 2016, **37**, 2365-2378.
22. Ramesh, J., Huleihel, M., Mordechai, J., Moser, A., Erukhimovich, V., Levi C., Kapelushnik, J., and Mordechai, S. *J Lab Clin Med*, 2003, **141**, 385-394.
23. Sahu, R. K., Zelig, U., Huleihel, M., Brosh, N., Talyshinsky, M., Ben-Harosh, M., Mordechai, S., and Kapelushnik, J. *Leuk Res*, 2006, **30**, 687-693.
24. González-Solís, J. L., Martínez-Espinosa, J. C., Salgado-Román, J. M., and Palomares-Anda, P. *Lasers Med Sci*, 2014, **29**, 1241-1249.
25. Bellisola, G., Cinque, G., Vezzalini, M., Moratti, E., Silvestri, G., Redaelli, S., Gambacorti-Passerini, C., Wehbe, K., and Sorio, C. *Analyst*, 2013, **138**, 3934-3945.

26. Rutter, A. V., Siddique, M. R., Filik, J., Sandt, C., Dumas, P., Cinque, G., Sockalingum, G. D., Yang, Y., and Sulé-Suso, J. *Cytometry Part A*, 2014, **85A**, 688-697.

27. Burke, J. R. *J Biol Chem*, 2003, **278**, 1450-1456.

28. Weisberg, E., Manley, P., Mestan, J., Cowan-Jacob, S., Ray, A., and Griffin, J. D. *Br J Cancer*, 2006, **94**, 1765-1769.

29. Kantarjian, H. M., Hochhaus, A., Saglio, G., De Souza, C., Flinn, I. W., Stenke, L., Goh, Y. T., Rosti, G., Nakamae, H., Gallagher, N. J., Hoenekopp, A., Blakesley, R. E., Larson, R. A., and Hughes, T. P. *Lancet Oncol*, 2011, **12**, 841-851.

30. Weisberg, E., Manley, P. W., Breitenstein, W., Brüggen, J., Cowan-Jacob, S. W., Ray, A., Huntly, B., Fabbro, D., Fendrich, G., Hall-Meyers, E., Kung, A. L., Mestan, J., Daley, G. Q., Callahan, L., Catley, L., Cavazza, C., Azam, M., Neuberg, D., Wright, R. D., Gilliland, D. G., and Griffin, J. D. *Cancer Cell*, 2005, **7**, 129-141.

31. Pijanka, J., Kohler, A., Yang, Y., Dumas, P., Chio-Srichan, S., Manfait, M., Sockalingum, G. D., and Sulé-Suso, J. *Analyst*, 2009, **134**, 1176-1181.

32. Kohler, A., Sulé-Suso, J., Sockalingum, G. D., Tobin, M., Bahrami, F., Yang, Y., Pijanka, J., Dumas, P., Cotte, M., van Pittius, D. G., Parkes, G., and Martens, H. *Appl Spectrosc*, 2008, **62**, 259-266.

33. Pijanka, J. K., Stone, S., Rutter, A. V., Forsyth, N., Sockalingum, G. D., Yang, Y., and Sulé-Suso, J. *Analyst*, 2013, **138**, 5052-5058.

34. Jamin, N., Dumas, P., Moncuit, J., Fridman, W. H., Teillaud, J. L., Carr, G. L., and Williams, G. P. *Proc Natl Acad Sci USA*, 1998, **95**, 4837-4840.
35. Holman, H. Y. N., Martin, M. C, Blakely, E. A., Bjornstad, K., and McKinney, W. R. *Biopolymers*, 2000, **57**, 329-335.
36. Zhou, J., Wang, Z., Sun, S., Liu, M., and Zhang, H. *Biotechnol Appl Biochem*, 2001, **33**, 127-132.
37. Gasper, R., Dewelle, J., Kiss, R., Mijatovic, T., and Goormaghtigh, E. *Biochim Biophys Acta*, 2009, **1788**, 1263-1270.
38. Liu, K. Z., and Mantsch, H. H. *J Mol Struct*, 2001, **565-566**, 299-304.
39. Zelig, U., Kapelushnik, J., Moreh, R., Mordechai, S., and Nathan, I. *Biophys J*, 2009, **97**, 2107-2114.
40. Liu, K.-Z., Shi, M.-H., and Mantsch, H. H. *Blood Cells Mol Dis*, 2005, **35**, 404-412.
41. Gasparri, F., and Muzio, M. *Biochem J*, 2003, **369**, 239-248.
42. Mahadevan-Jansen, A., Mitchell, M. F., Ramanujam, N., Malpica, A., Thomsen, S., Utzinger, U., Richards-Kortum, R., Malpica, A., Thomsen, S., Utzinger, U., and Richards-Kortum, R. l. *Photochem Photobiol*, 1998, **68**, 123-132.
43. Huang, Z., McWilliams, A., Lui, H., McLean, D. I., Lam, S., and Zeng, H. *Int J Cancer*, 2003, **107**, 1047-1052.
44. Tang, H.-W., Yang, X. B., Kirkham, J., and Smith, D. A. *Anal Chem*, 2007, **79**, 3646-3653.
45. Chowdary, M. V., Kumar, K. K., Kurien, J., Mathew, S., and Krishna, C. M. *Biopolymers*, 2006, **83**, 556-569.

46. Tze-Chien C., Ming-Chih Y., Chih-Chiang C., Ming-Shun W., Yu-Chieh L., and Yen-Chou C. *Toxicol in Vitro*, 2016, **31**, 1-11.

Legends to Figures

Figure 1. S-FTIR spectra of clone 4F (resistant to both 50 μM and 100 μM of nilotinib) in the presence and absence of nilotinib. Each spectrum is the mean of 50 individual spectra from 50 individual cells. Spectra are offset for clarity.

Figure 2. S-FTIR spectra of clone 7F (partially sensitive to 50 μM of nilotinib) in the presence and absence of nilotinib. The spectra are the mean of 50 individual spectra from 50 individual cells (0 μM) and the mean of 23 individual spectra from 23 individual cells (50 μM). Spectra are offset for clarity.

Figure 3. PCA of FTIR spectra of clone 4F (resistant to both 50 and 100 μM of nilotinib) for cells incubated with 0 μM nilotinib (circles), 50 μM nilotinib (triangles), and 100 μM nilotinib (crosses) for fingerprint (A) and lipid (C) regions and loading plots, respectively (B and D).

Figure 4. PCA of FTIR spectra of clone 7F (partially sensitive to 50 μM of nilotinib) for cells incubated with 0 μM nilotinib (circles) and 50 μM nilotinib (triangles) for (fingerprint (A) and lipid (C) regions and loading plots, respectively (B and D).

Figure 5. PCA of FTIR spectra of control cells (incubated with 0 μM nilotinib) of sensitive and resistant study clones for fingerprint (A) and lipid (C) regions and loading plots, respectively (B and D). See main text for data labelling.

Figure 6. Raman spectra of clone 1Ra (resistant to both 50 μM and 100 μM of nilotinib) in the presence and absence of nilotinib. Each spectrum is the mean of 50 individual spectra from 50 individual cells. Spectra are offset for clarity.

Figure 7. Raman spectra of clone 2Ra (partially sensitive to 50 μM of nilotinib) in the presence and absence of nilotinib. The spectra are the mean of 50 individual spectra from 50 individual cells (0 μM) and the mean of 25 individual spectra from 25 individual cells (50 μM). Spectra are offset for clarity.

Figure 8. PCA of Raman spectra (A) and loading plot (B) of clone 1Ra (resistant to both 50 μM and 100 μM of nilotinib) for cells incubated with 0 μM nilotinib (circles), 50 μM nilotinib (triangles), and 100 μM nilotinib (crosses).

Figure 9. PCA of Raman spectra (A) and loading plot (B) of clone 2Ra (partially sensitive to 50 μM of nilotinib) for cells incubated with 0 μM nilotinib (circles) and 50 μM nilotinib (triangles).

Figure 1.

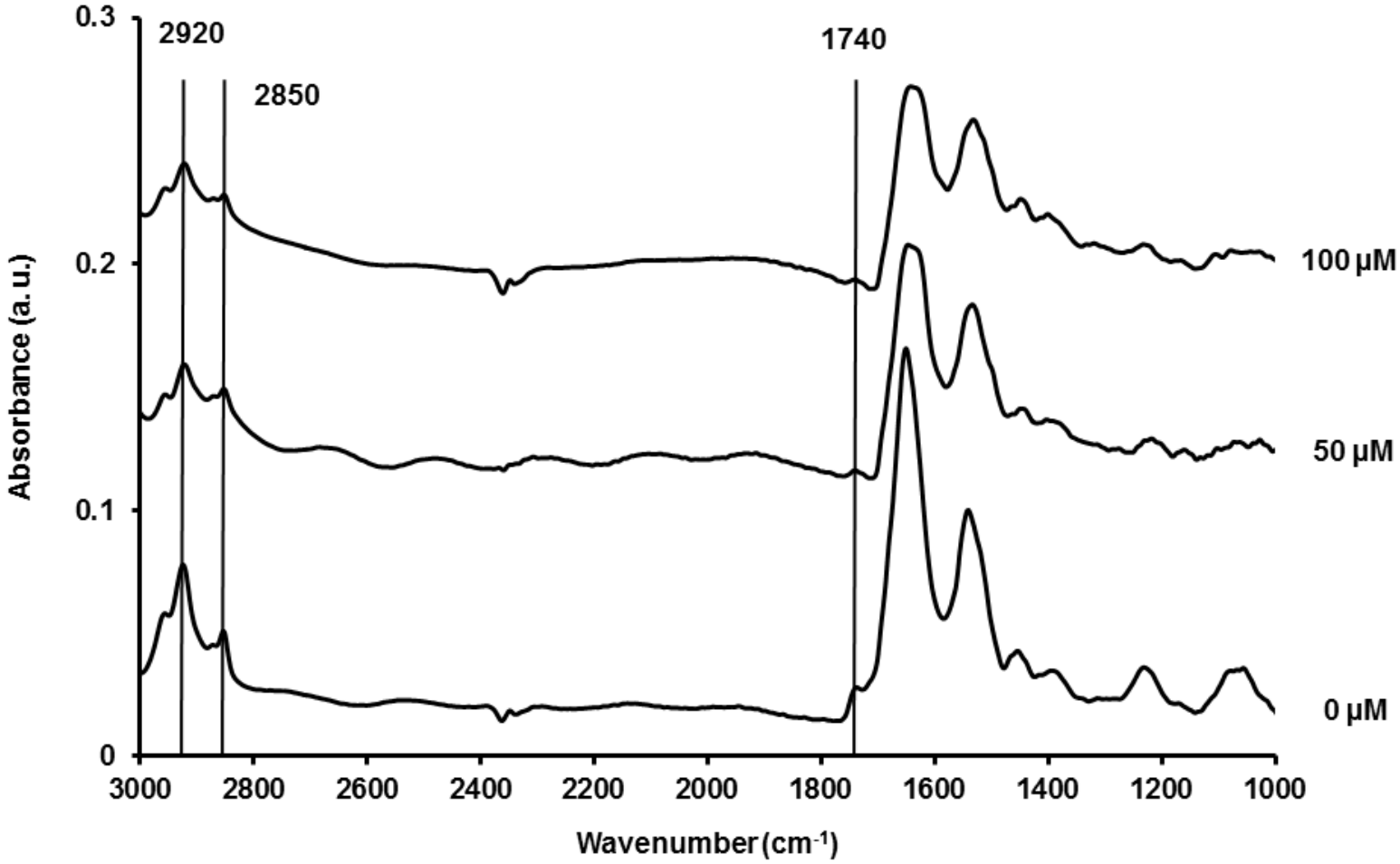
0.3
0.2
0.1
0
Absorbance (a. u.)
2920
2850
1740
100 µM
50 µM
0 µM
3000
2800
2600
2400
2200
2000
1800
1600
1400
1200
1000
Wavenumber (cm-1)

Figure 2.

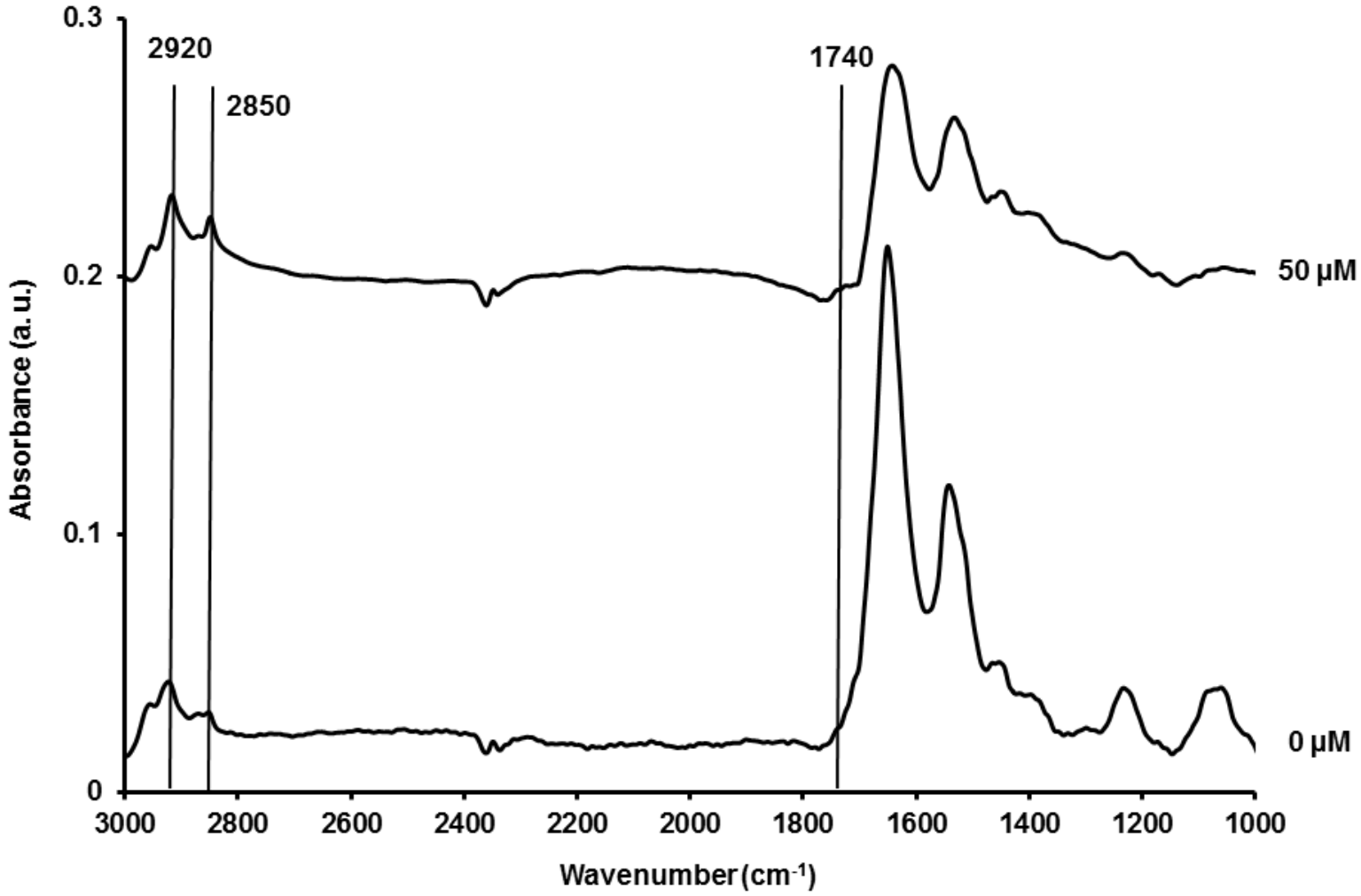
0.3
0.2
0.1
0
Absorbance (a. u.)
2920
2850
1740
50 µM
0 µM
3000
2800
2600
2400
2200
2000
1800
1600
1400
1200
1000
Wavenumber (cm-1)

Figure 3 A.

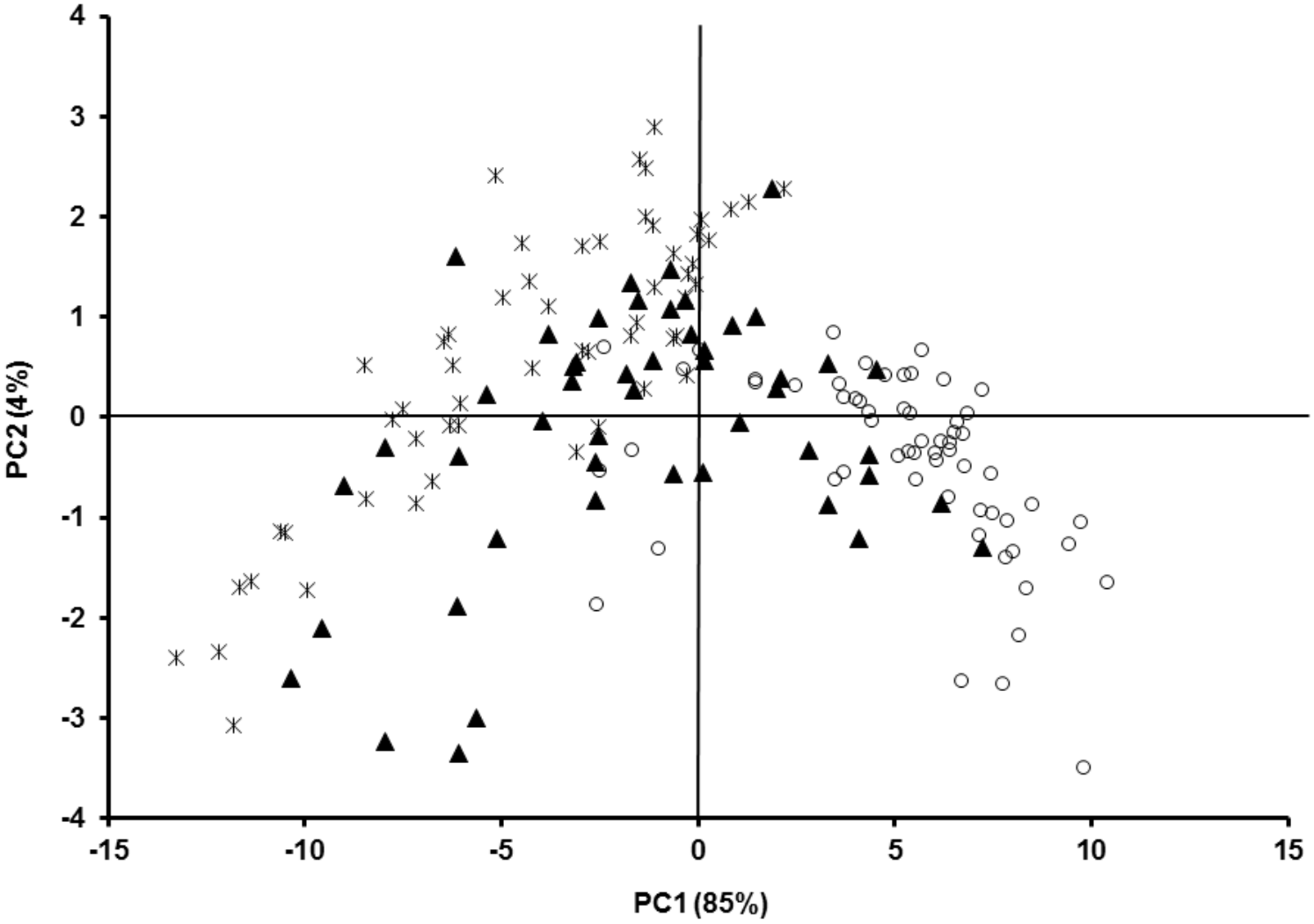

Figure 3 B.

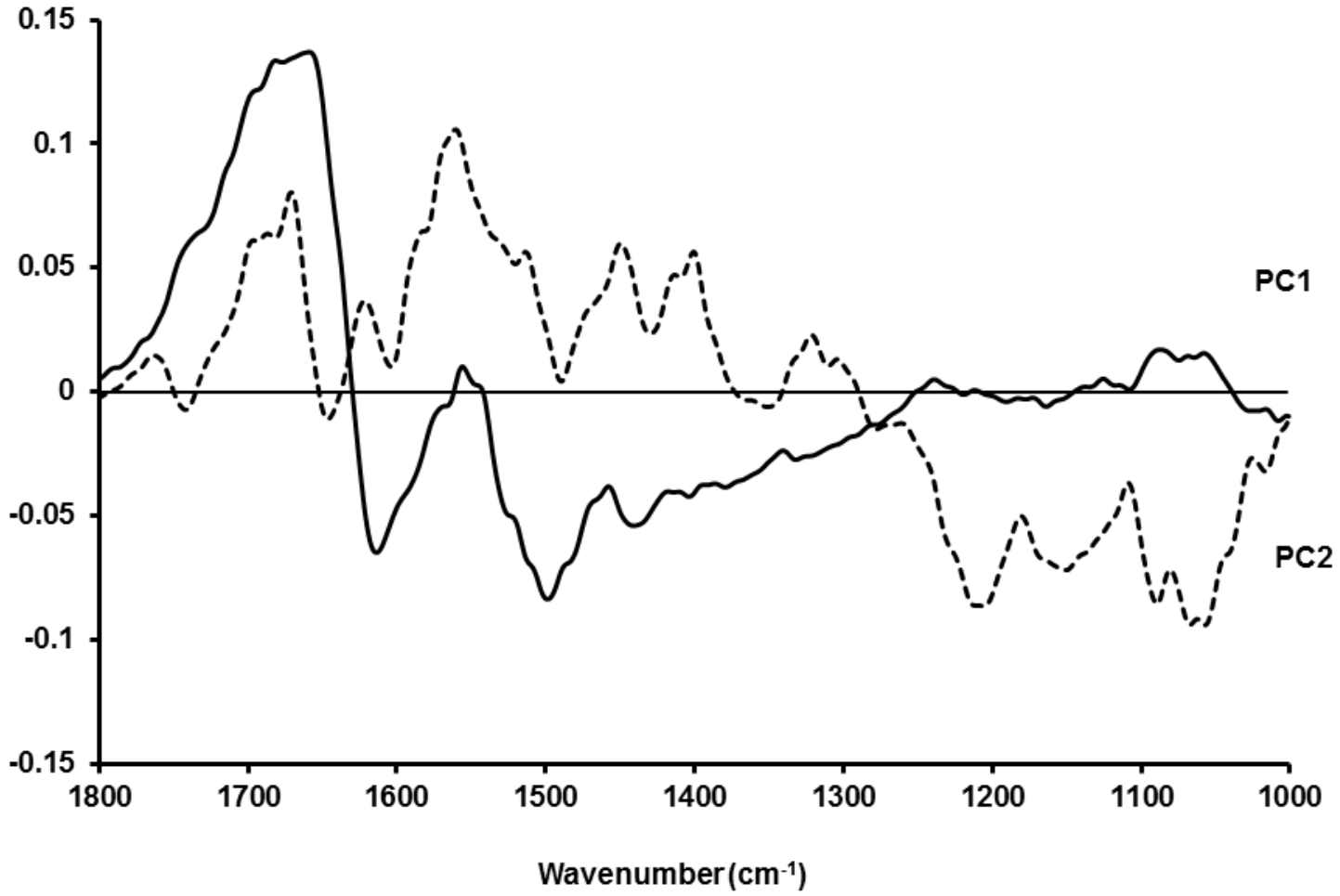
0.15
0.1
0.05
0
-0.05
-0.1
-0.15
1800
1700
1600
1500
1400
1300
1200
1100
1000
PC1
PC2
Wavenumber (cm-1)

Figure 3 C.

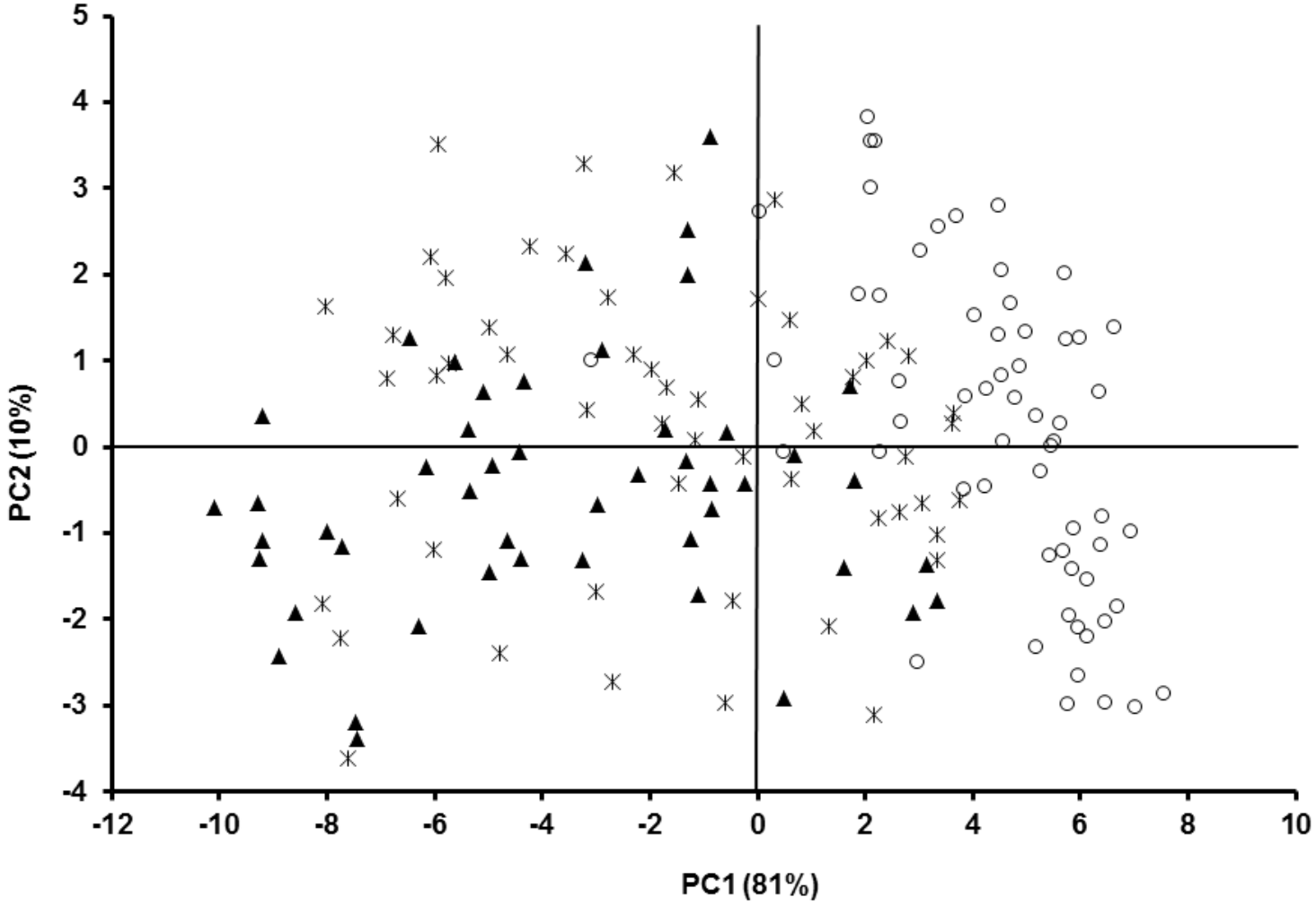

Figure 3 D.

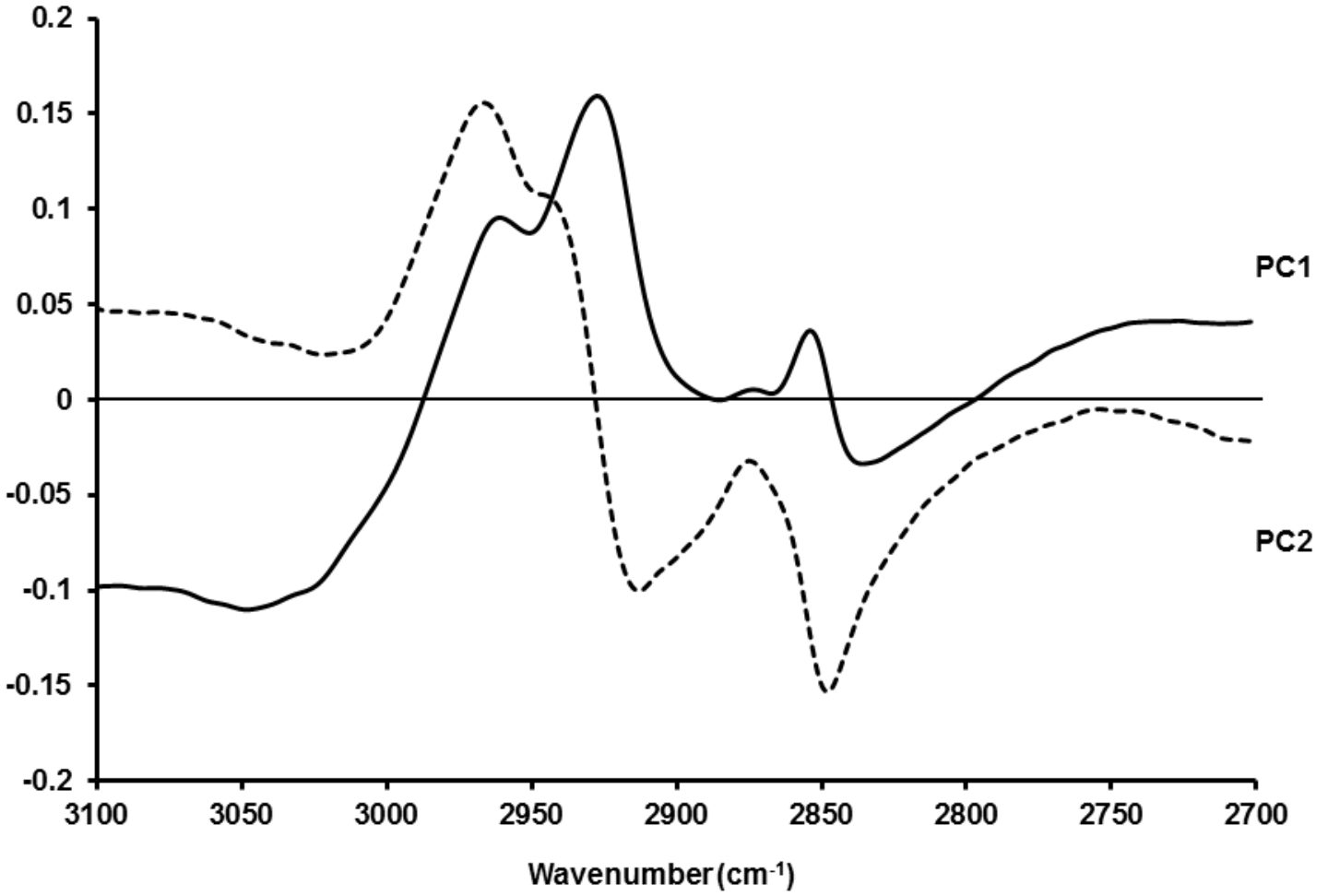
0.2
0.15
0.1
0.05
0
-0.05
-0.1
-0.15
-0.2
3100
3050
3000
2950
2900
2850
2800
2750
2700
Wavenumber (cm-1)
PC1
PC2

Figure 4 A.

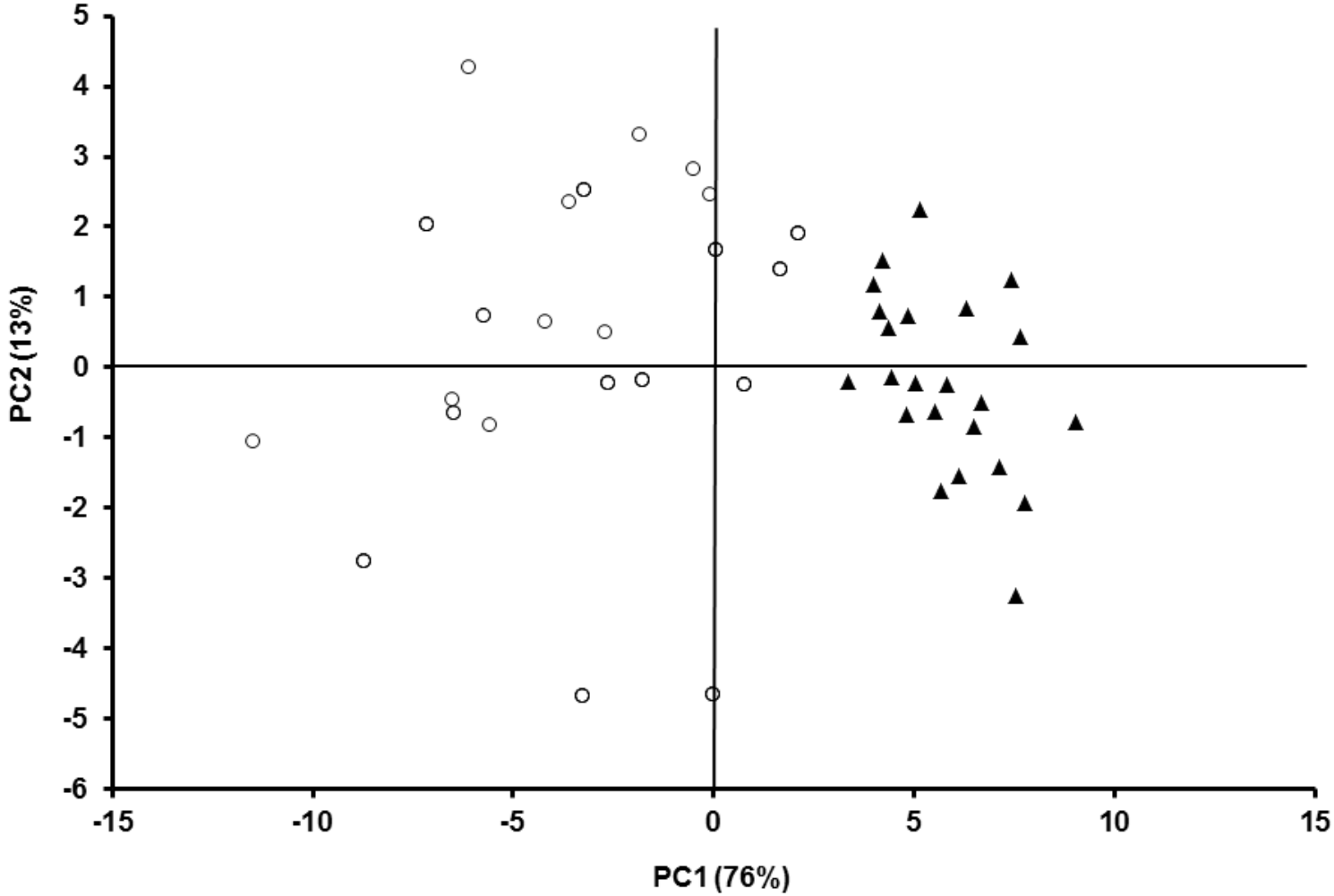

Figure 4 B.

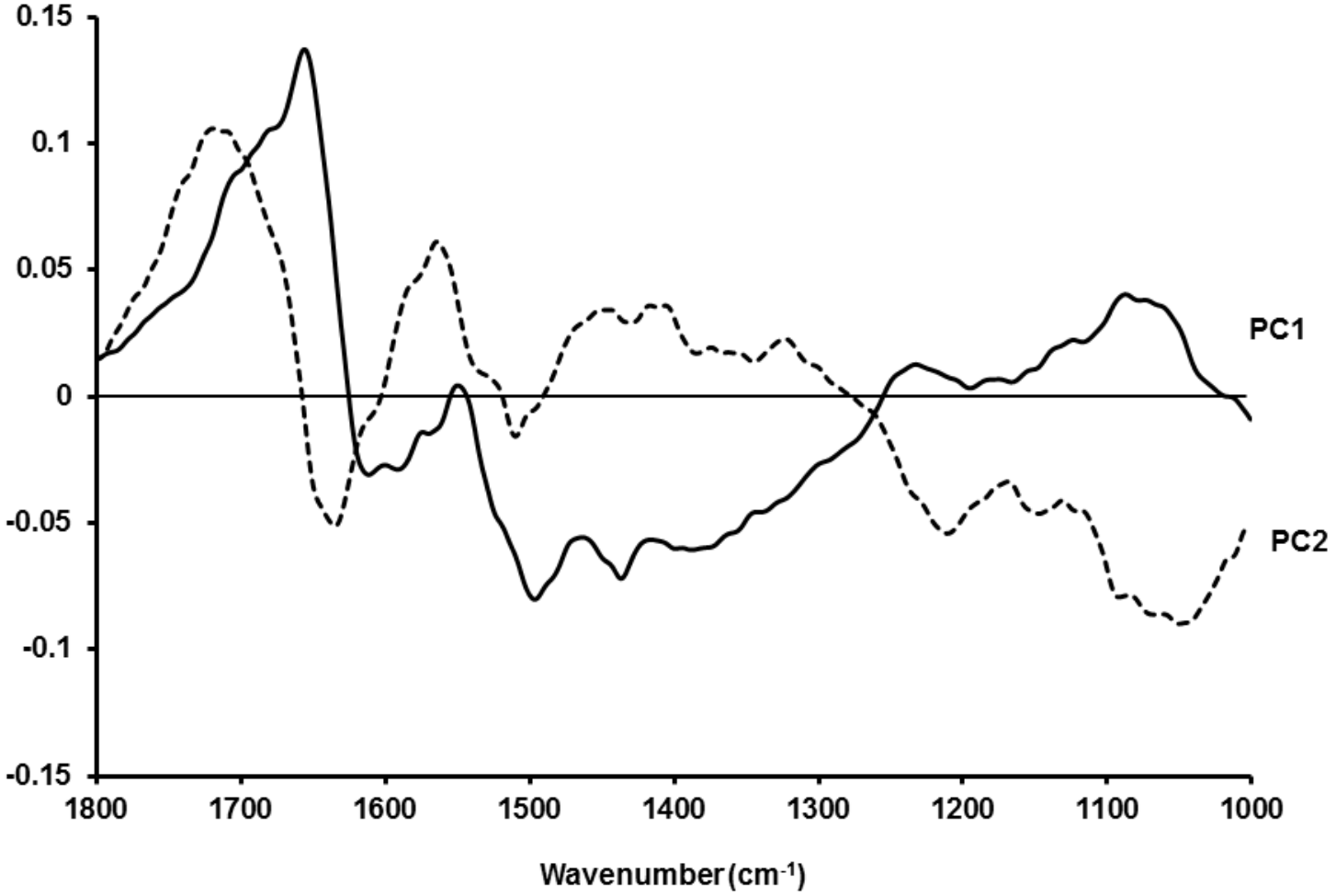
0.15
0.1
0.05
0
-0.05
-0.1
-0.15
1800
1700
1600
1500
1400
1300
1200
1100
1000
PC1
PC2
Wavenumber (cm-1)

Figure 4 C

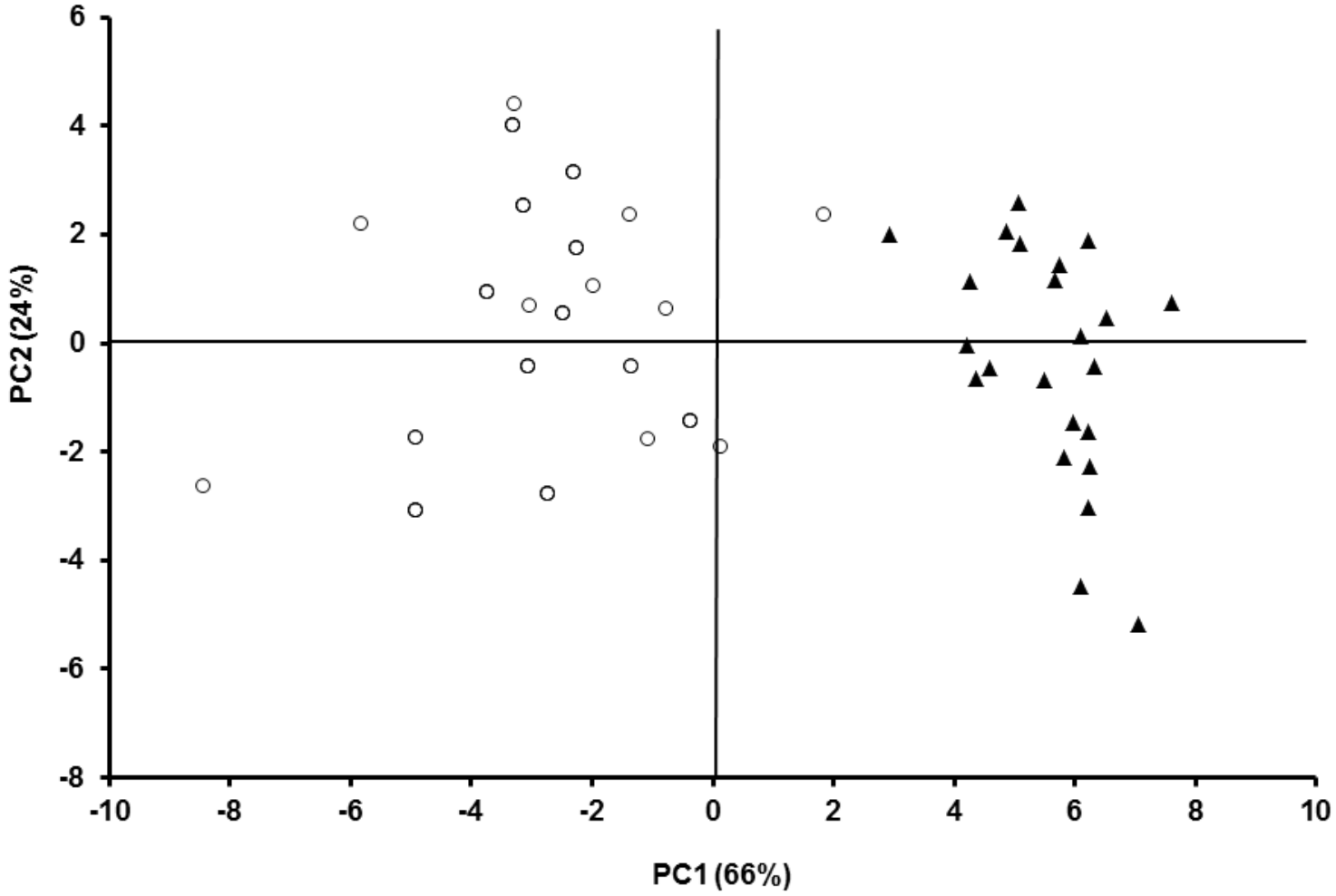

Figure 4 D.

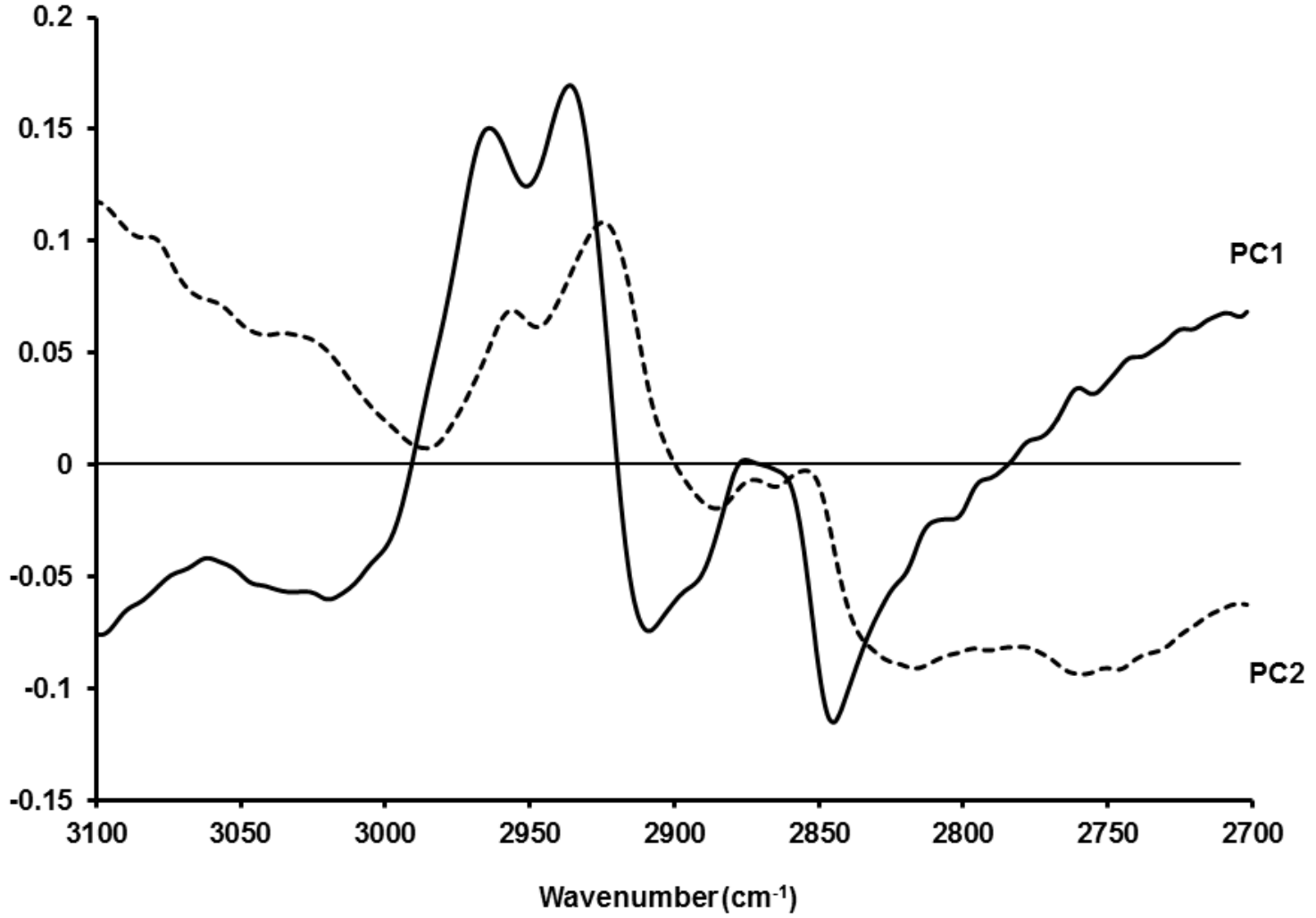
0.2
0.15
0.1
0.05
0
-0.05
-0.1
-0.15
3100
3050
3000
2950
2900
2850
2800
2750
2700
PC1
PC2
Wavenumber (cm-1)

Figure 5 A.

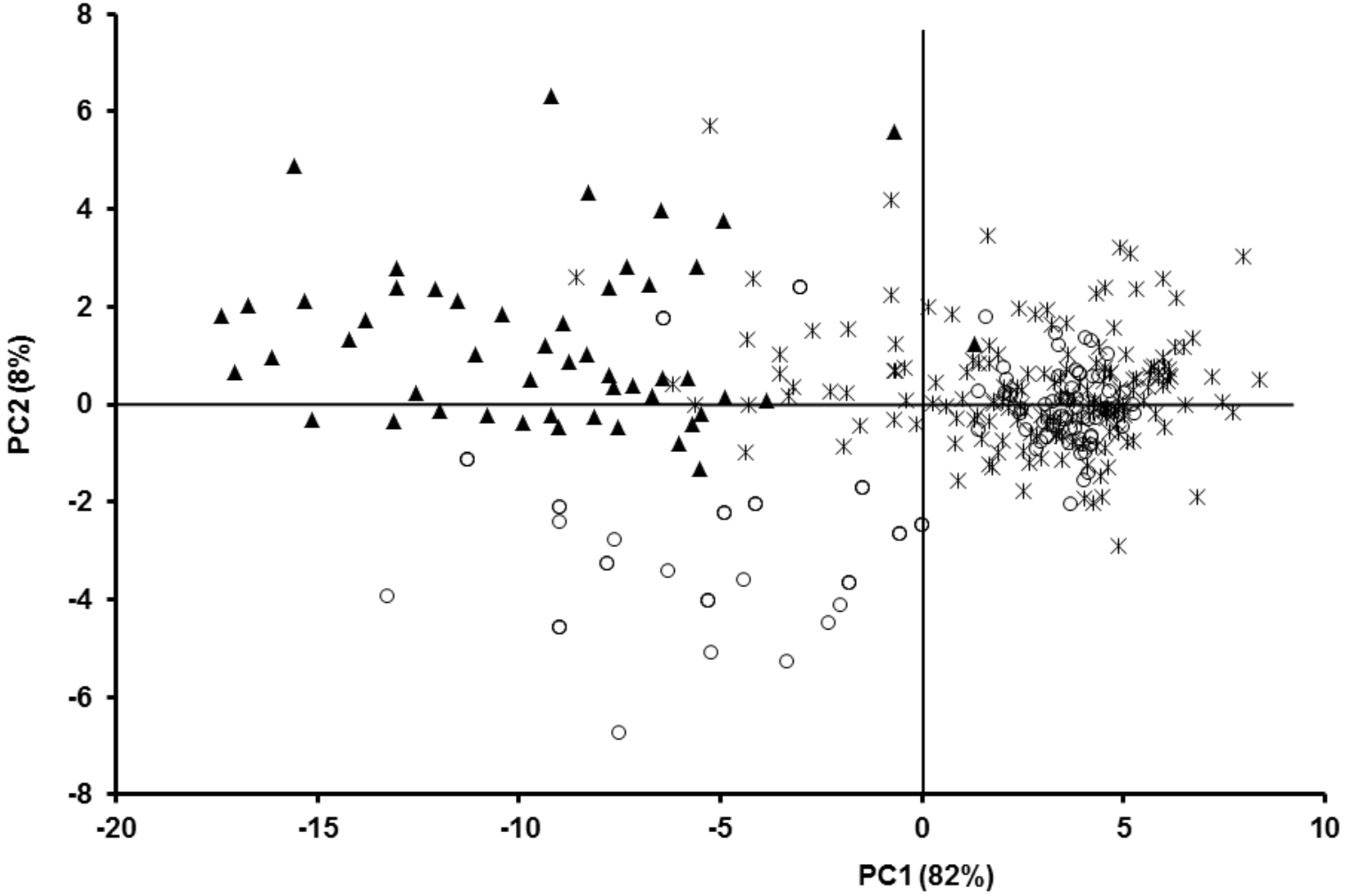

Figure 5 B.

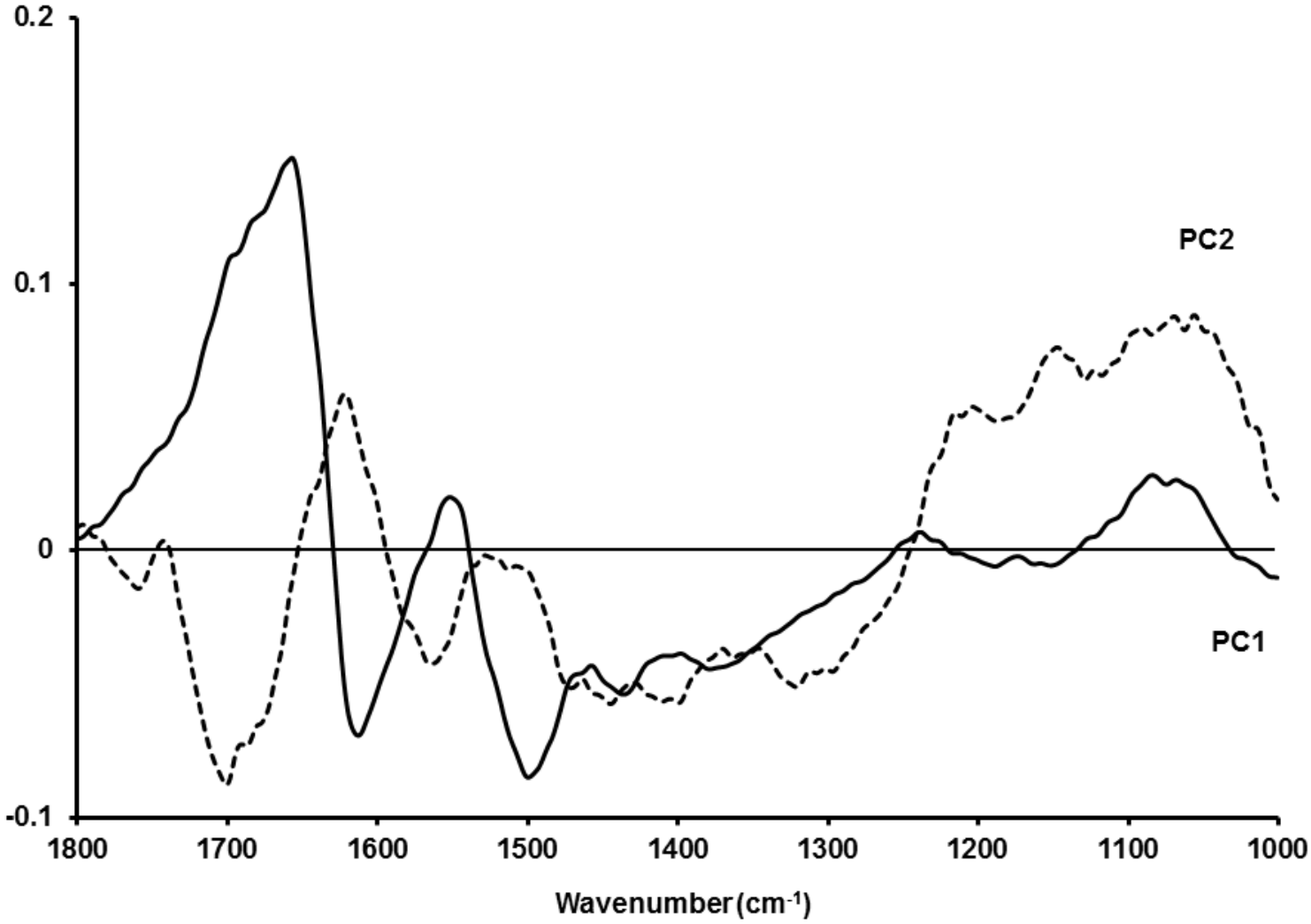
0.2
0.1
0
-0.1
1800
1700
1600
1500
1400
1300
1200
1100
1000
Wavenumber (cm-1)
PC2
PC1

Figure 5 C.

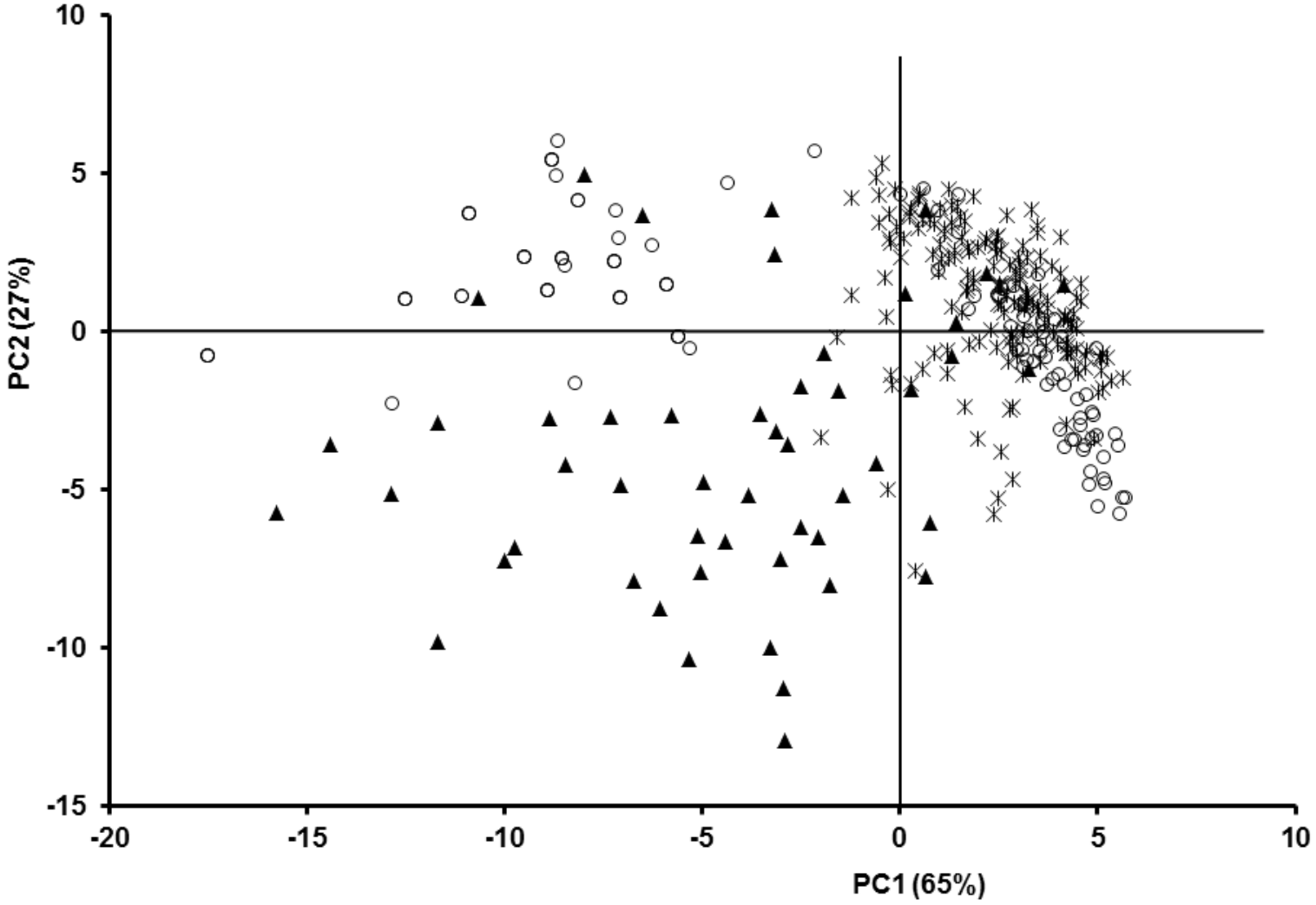

Figure 5 D.

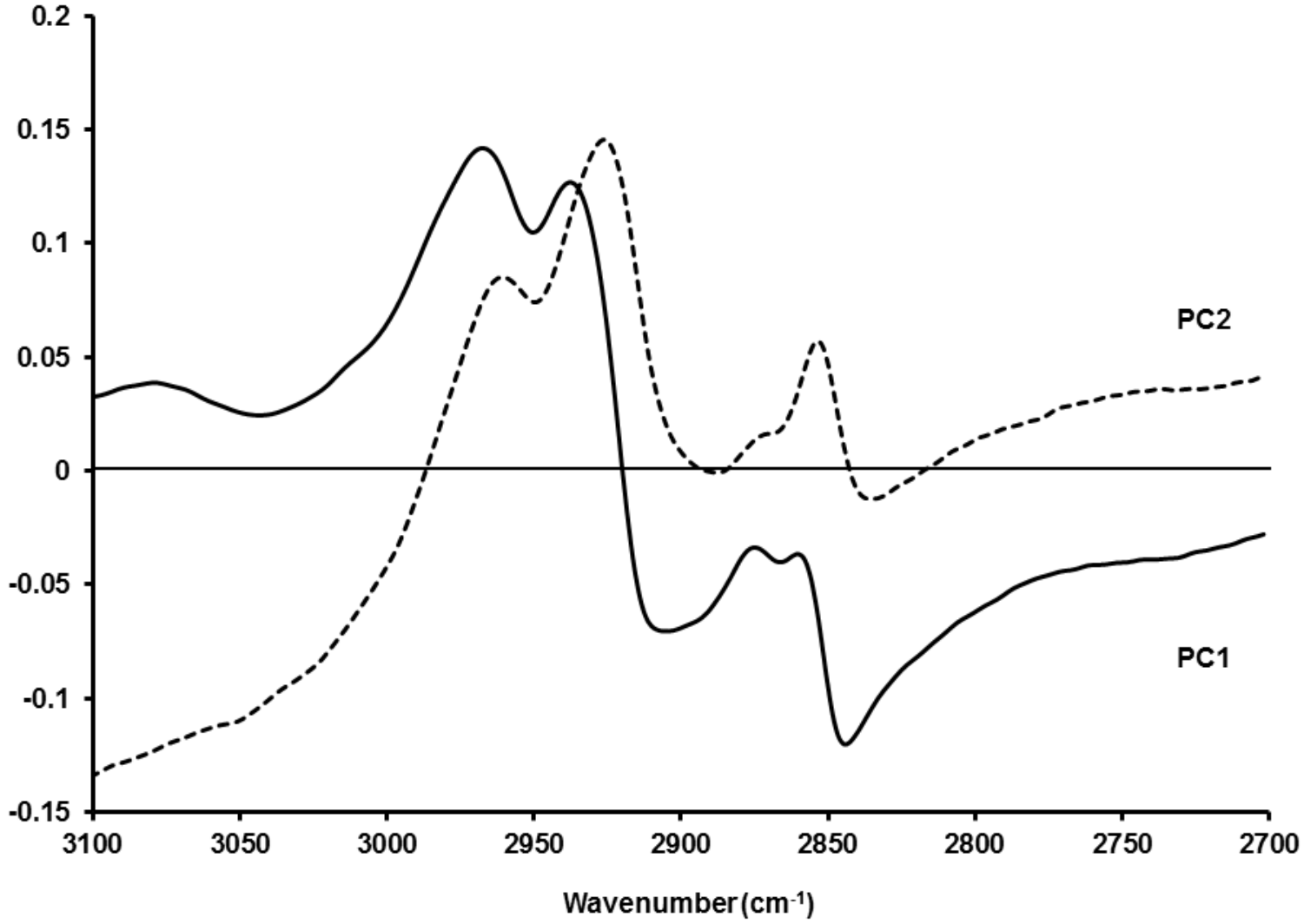
0.2
0.15
0.1
0.05
0
-0.05
-0.1
-0.15
3100
3050
3000
2950
2900
2850
2800
2750
2700
PC2
PC1
Wavenumber (cm-1)

Figure 6.

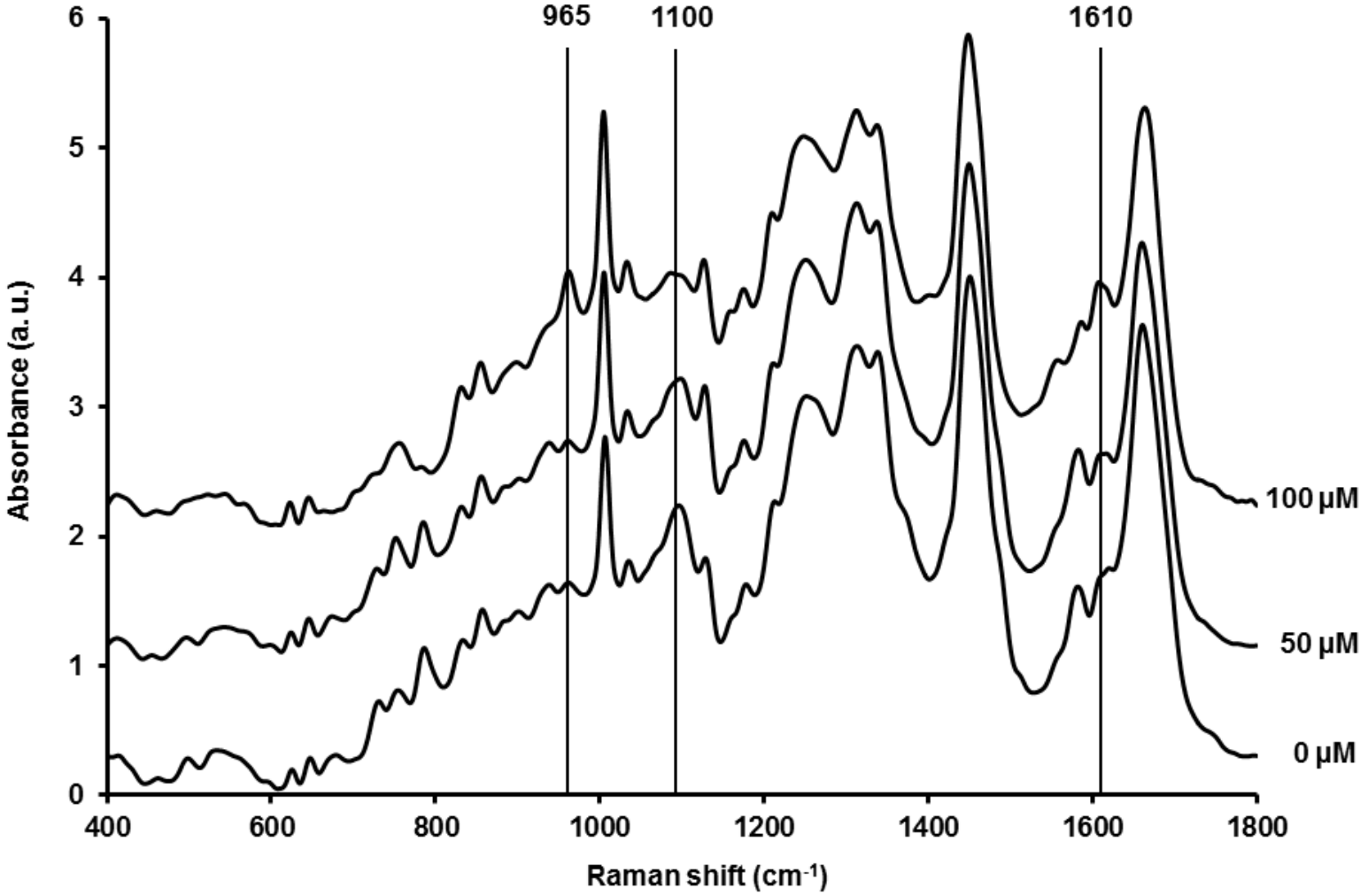
965
1100
1610
6
5
4
3
2
1
0
Absorbance (a.u.)
400
600
800
1000
1200
1400
1600
1800
Raman shift (cm-1)
100 µM
50 µM
0 µM

Figure 7.

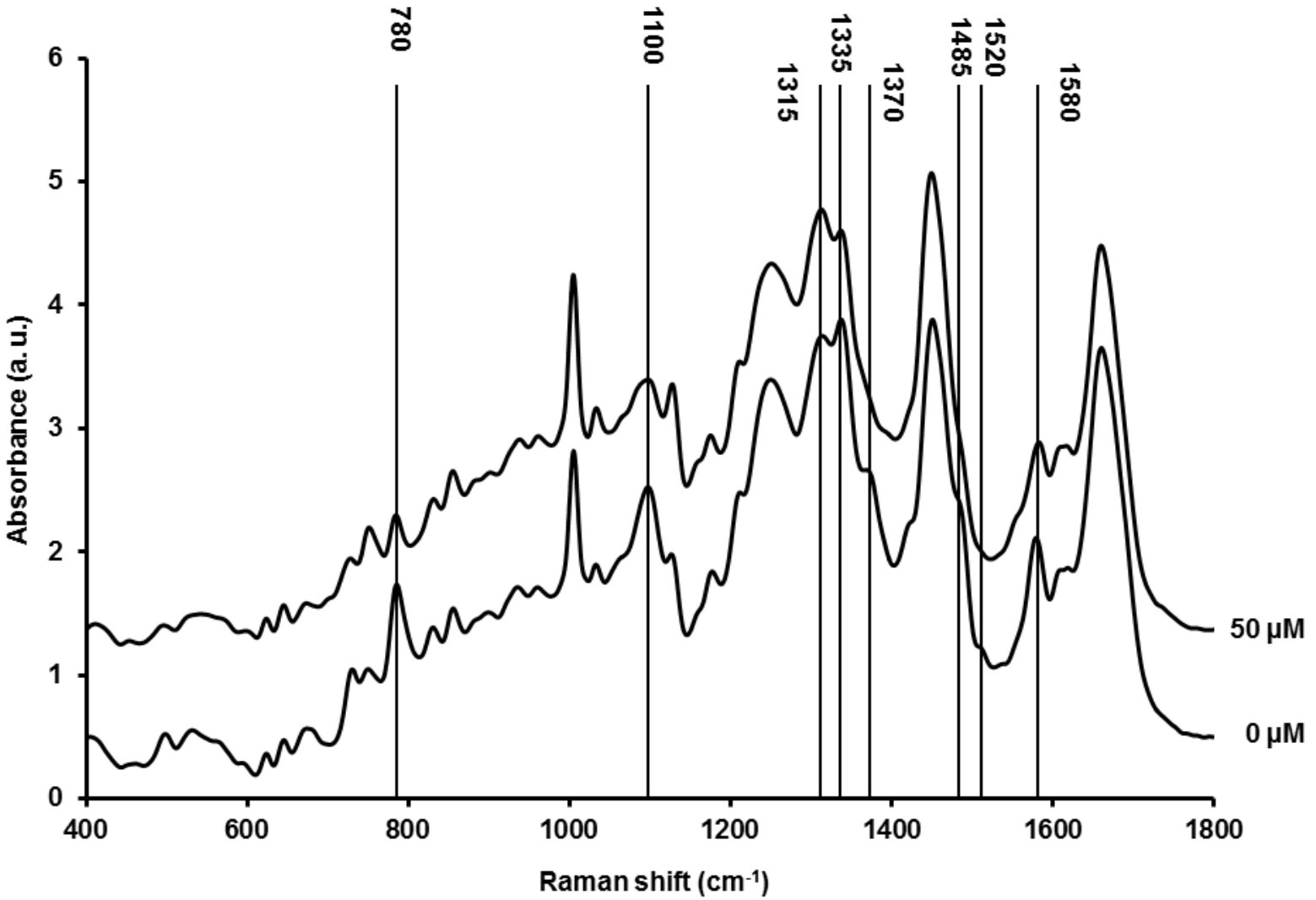
780
1100
1315
1335
1370
1485
1520
1580
Absorbance (a.u.)
Raman shift (cm-1)
50 µM
0 µM
0
1
2
3
4
5
6
400
600
800
1000
1200
1400
1600
1800

Figure 8 A.

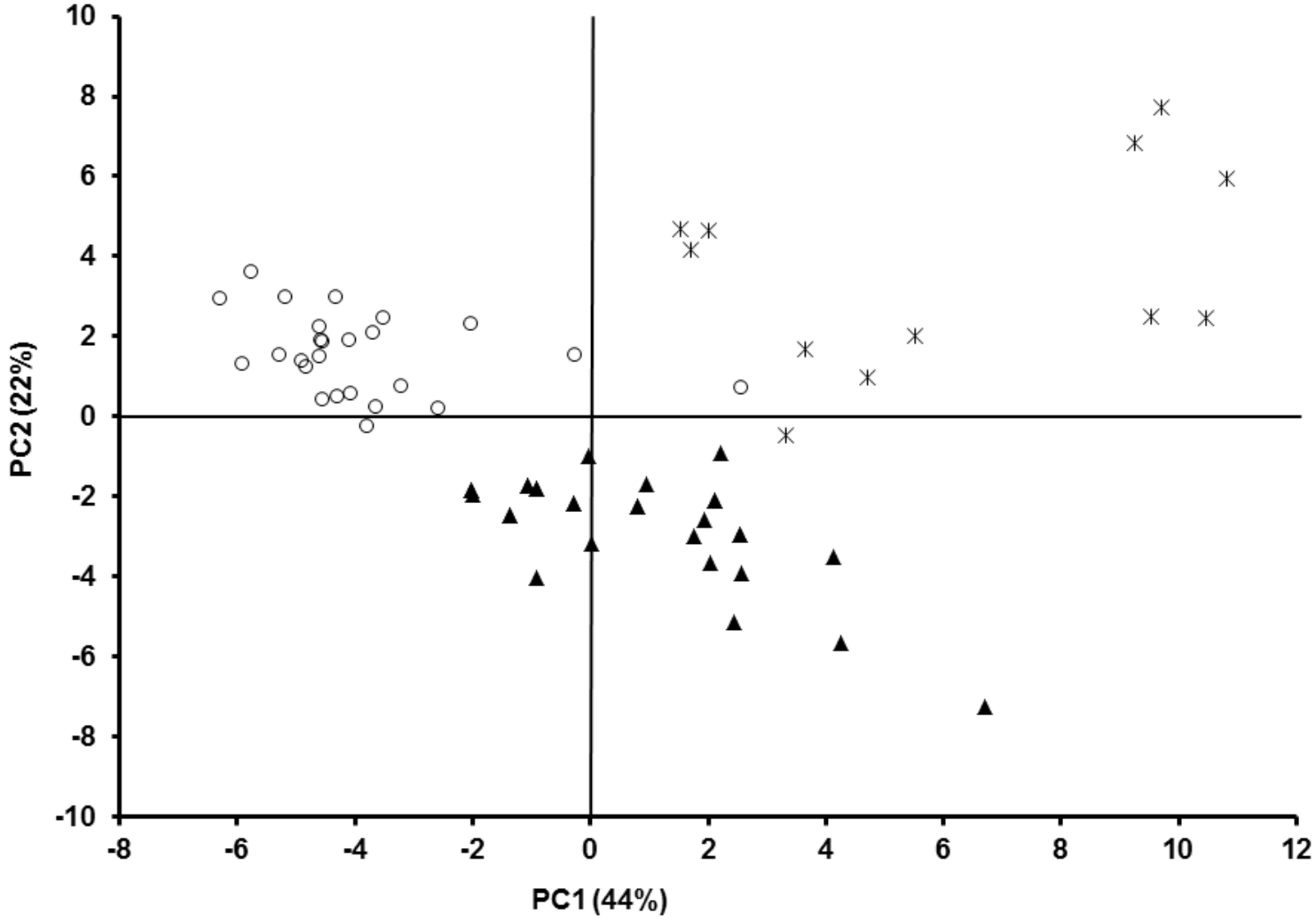

Figure 8 B.

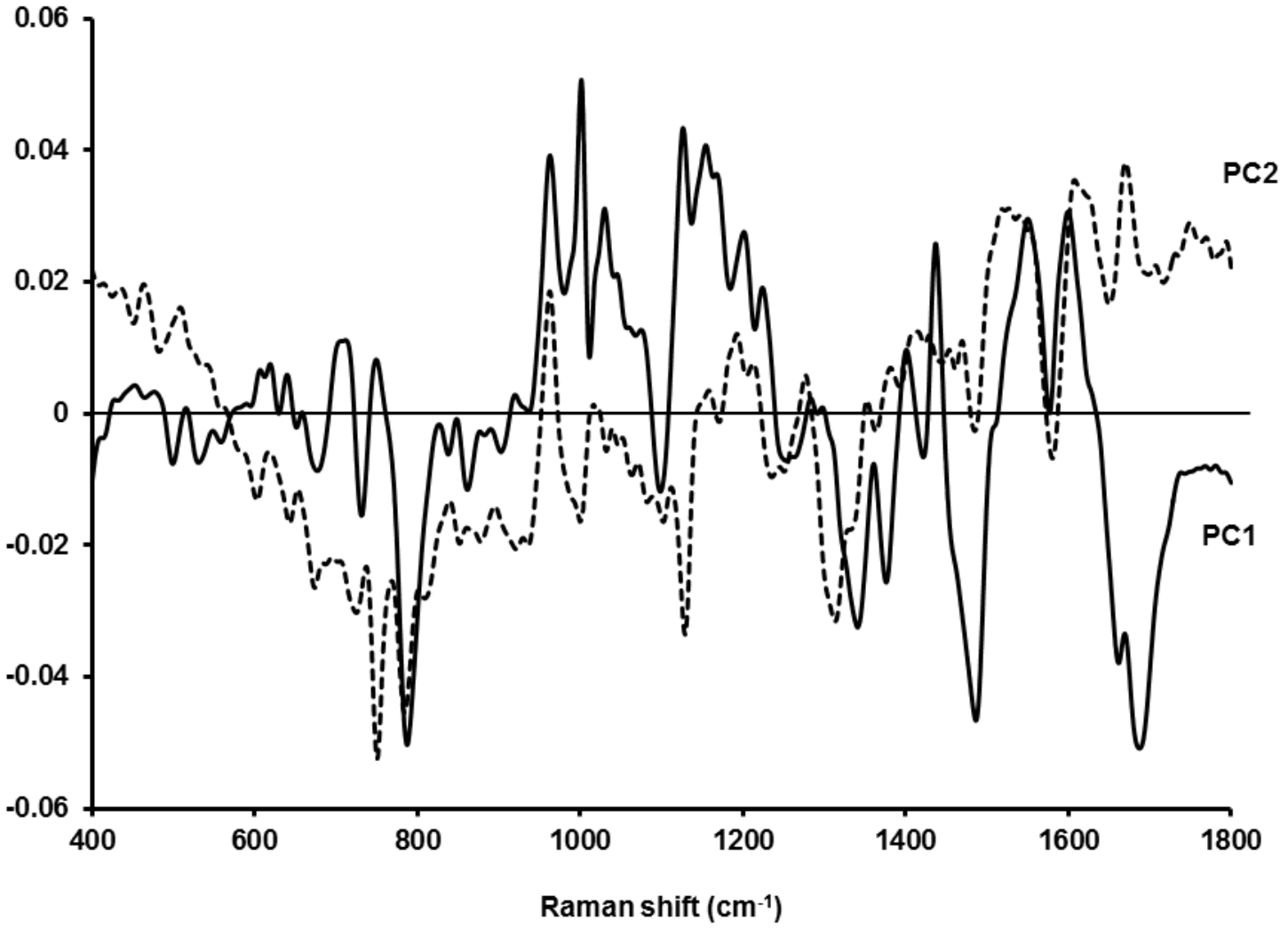
0.06
0.04
0.02
0
-0.02
-0.04
-0.06
400
600
800
1000
1200
1400
1600
1800
PC2
PC1
Raman shift (cm-1)

Figure 9 A.

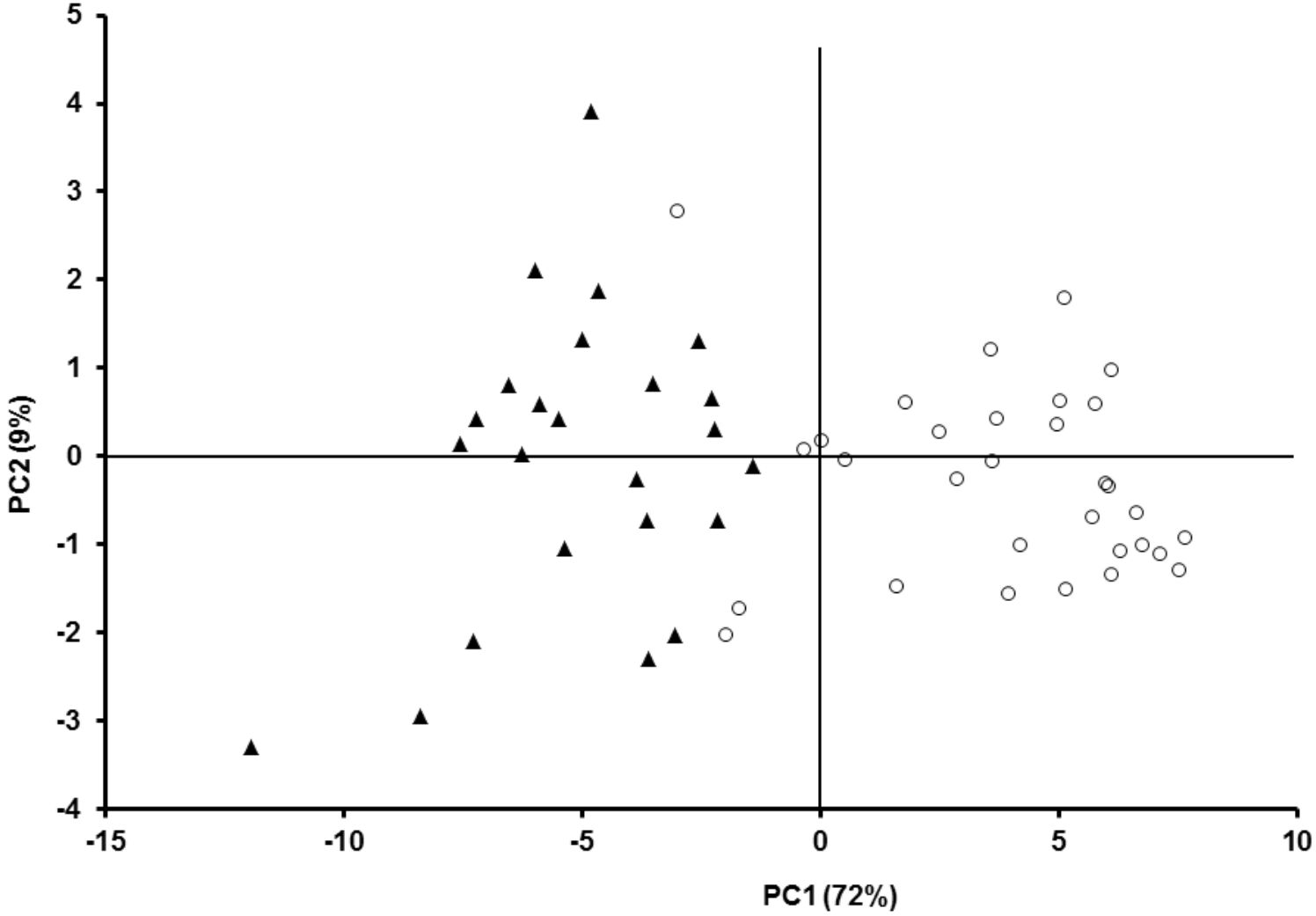

Figure 9 B.

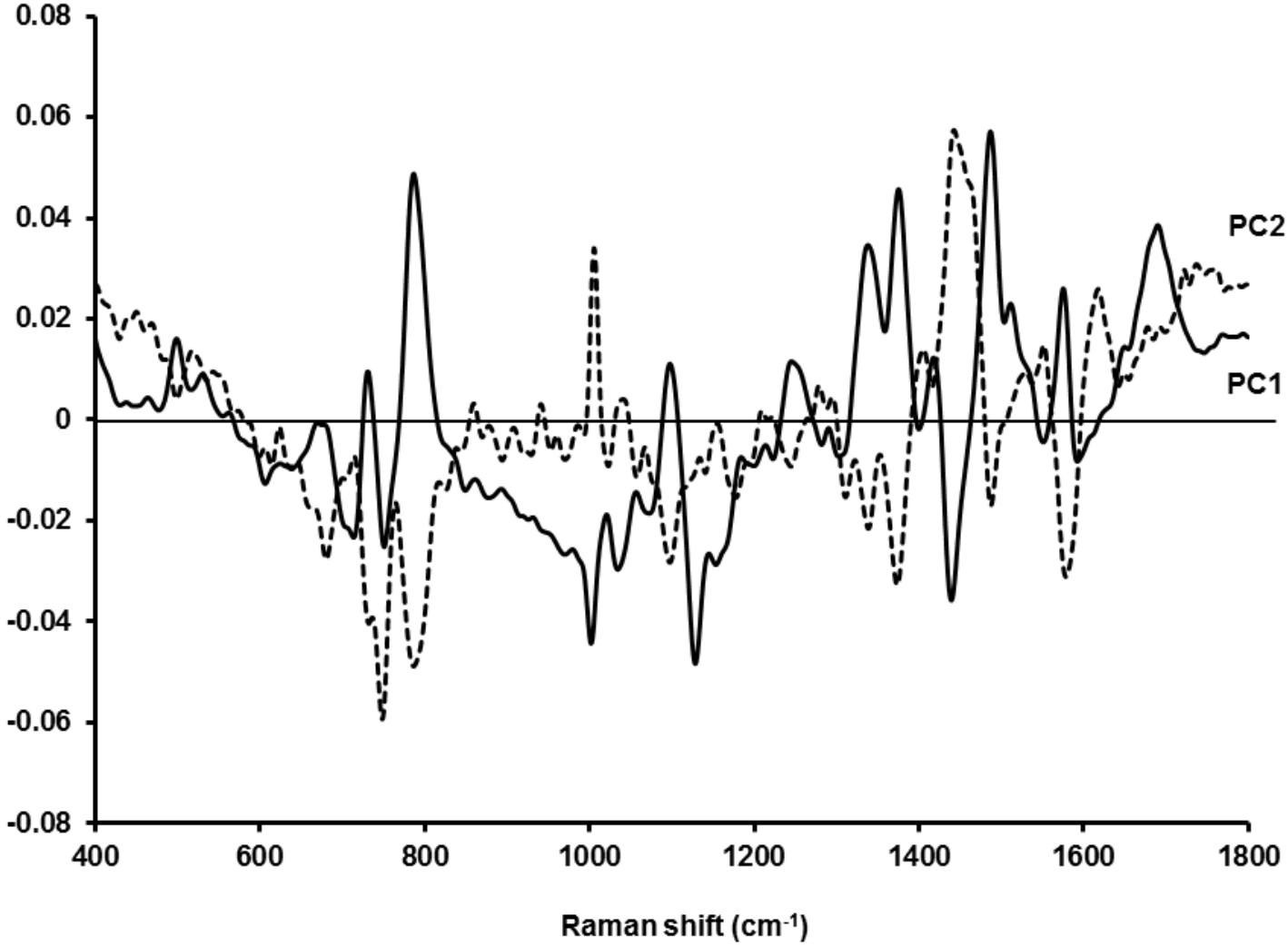
0.08
0.06
0.04
0.02
0
-0.02
-0.04
-0.06
-0.08
400
600
800
1000
1200
1400
1600
1800
PC2
PC1
Raman shift (cm-1)

Table I: Representative example of K562 cell clones following 5 days incubation with nilotinib at different doses.

Clones	Control (0 μM)	50 μM	100 μM
1	++	+/-	+/-
2	++	+	++
3	++	+	+/-
4	++	+	+
5	++	+	+
6	++	+	+
7	++	+	+
8	++	+	+
9	++	+	+
10	++	+	+
11	++	+	+/-
12	++	+	+
13	+-	+/-	+/-
14	++	+/-	+/-
15	++	+	+
16	++	+/-	-
17	++	+/-	+/-
18	++	+/-	-